Quaternary Science Advances 14 (2024) 100186

Contents lists available at ScienceDirect

Quaternary Science Advances

journal homepage: www.sciencedirect.com/journal/quaternary-science-advances

Explosive volcanic activity in Central-Southern Italy during Middle Pleistocene: A tale from tephra layers of the Acerno basin

C. Pelullo [a,**], I. Arienzo [a], M. D'Antonio [b], B. Giaccio [c,d], R.S. Iovine [a], N. Leicher [e], D.M. Palladino [f], M. Petrelli [g], P. Petrosino [b,*], E. Russo Ermolli [b], G. Sottili [f], F. Totaro [b], G. Zanchetta [d,h]

[a] Istituto Nazionale di Geofisica e Vulcanologia, Osservatorio Vesuviano, Via Diocleziano, 328, 80124, Naples, Italy
[b] Dipartimento di Scienze della Terra, dell'Ambiente e delle Risorse, Università di Napoli Federico II, Via Vicinale Cupa Cintia, 21, 80126, Naples, Italy
[c] Istituto di Geologia Ambientale e Geoingegneria – CNR, Via Salaria km 29.300, Monterotondo, Rome, Italy
[d] Istituto Nazionale di Geofisica e Vulcanologia, Via di Vigna Murata, 605, 00143, Rome, Italy
[e] Institute of Geology and Mineralogy, University of Cologne, Zuelpicher Str. 49a, 50674, Cologne, Germany
[f] Dipartimento di Scienze della Terra, Sapienza-Università di Roma, Piazzale Aldo Moro, 5, 00185, Rome, Italy
[g] Dipartimento di Fisica e Geologia, Università di Perugia, Piazza Università, 1, 06100, Perugia, Italy
[h] Dipartimento di Scienze della Terra, Università di Pisa, Via Santa Maria, 53, 56126, Pisa, Italy

ARTICLE INFO

Keywords:
Tephrostratigraphy
Acerno basin
Peri-Tyrrhenian Italian volcanoes
Middle Pleistocene
Trace elements
Sr and Nd isotopes

ABSTRACT

The cored succession of the Acerno basin, a tectonic palaeolake located in the southern Apennines (Italy), represents a key point of the Italian tephrostratigraphic network for the Quaternary. Trace element and isotope ($^{87}Sr/^{86}Sr$ and $^{143}Nd/^{144}Nd$) data have been acquired on bulk rock, glassy groundmass and separated minerals (feldspar and pyroxene phenocrysts) from twenty-one tephra layers, dated between ~570 and 470 ka, embedded in the lacustrine sediments of the basin. The already available major element compositions have been here combined with the newly acquired data. The whole dataset provides a full geochemical characterization of the tephra that strengthens and improves previous attempts to identify their volcanic sources and potential correlatives. In this context, several previously proposed correlations among distal archives have been here confuted. The geochemical fingerprints highlight that the volcanic record preserved in the Acerno lacustrine succession can be attributed to the explosive activity of the Roccamonfina, Colli Albani, Sabatini, Pontian islands (Latium region, Central Italy) and the Neapolitan Volcanic Area (Campania region, South Italy), providing new insights to enhance the current knowledge on the Middle Pleistocene volcanic record in Italy. Moreover, tephra attributions suggest still unknown eruptive activity of such volcanoes during the Quaternary. From this perspective, our study testifies how difficult it is to precisely correlate different geological archives even in a very short time interval. Such a difficulty arises from a large number of volcanic events concentrated in a relatively short time span, with products of similar chemical composition, and from the incomplete characterization of the successions in proximal outcrops. A thorough reconstruction of the eruptive history of these volcanic complexes requires a wider and denser study of distal archives, alongside further investigations in proximal areas.

1. Introduction

Explosive volcanism is responsible for the fragmentation of magma and transport into atmosphere of juvenile and lithic particles (tephra) that can be spread by wind over wide geographical areas and deposited in different sedimentary settings at considerable distances from the source. Nowadays, the importance of studying tephra from marine and terrestrial sedimentary successions and ice cores is widely recognized, as their identification improves knowledge on past volcanic activity and provides fundamental chronological information for a wide away of scientific issues, such as, paleoclimatic-environmental dynamics, archaeology and human evolution (e.g., Lowe and Hunt, 2001; Lowe, 2011; Davies, 2015; Giaccio et al., 2015, 2019; Regattieri et al., 2015; Lane et al., 2017; Petrelli et al., 2017; Zanchetta et al., 2018; Wagner

* Corresponding author.
** Corresponding author.
E-mail addresses: carlo.pelullo@unina.it (C. Pelullo), petrosin@unina.it (P. Petrosino).

https://doi.org/10.1016/j.qsa.2024.100186
Received 18 January 2024; Received in revised form 18 March 2024; Accepted 21 March 2024
Available online 4 April 2024

et al., 2019; Abbott et al., 2020; Vidal et al., 2022). Distal tephra deposits enable the characterization of old, major and/or minor volcanic events, often significant in terms of occurrence, erupted volumes and VEI (e.g., Giaccio et al., 2014). In addition, they can provide documentation of events that are not recorded in proximal (near-vent) settings, as they may be covered by the deposits of more recent eruptions or eroded. For these reasons, distal records allow a more complete reconstruction of the explosive volcanic history and provide further data needed for rigorous hazard assessment in active volcanic areas.

The Italian Peninsula is an ideal area for tephrostratigraphic research due to the conspicuous explosive activity of the peri-Tyrrhenian Quaternary volcanoes (e.g., Branca et al., 2023). Tephra layers are frequently found as event-layers in several sub-aerial, lacustrine and marine successions (e.g., Giaccio et al., 2017b and references therein). Specifically, Early to Late Pleistocene sedimentary successions from Central and Southern Italy are punctuated by tephra layers ascribed to different Italian eruptive centers, such as Vulsini, Vico, Sabatini, Colli Albani, Roccamonfina, Vulture, Somma-Vesuvius, Campi Flegrei, Ischia and Aeolian Islands (Fig. 1a; e.g., Keller et al., 1978; Paterne et al., 1986, 1988, 2008; Wulf et al., 2004, 2008; Bourne et al., 2010, 2015; Tamburrino et al., 2012; Insinga et al., 2014; Morabito et al., 2014; Petrosino et al., 2014b, 2015, 2016; D'Antonio et al., 2016; Giaccio et al., 2013a,b, 2014, 2015, 2019; Leicher et al., 2019, 2021, 2023; Regattieri et al., 2019; Monaco et al., 2021, 2022a; Totaro et al., 2022).

The Acerno basin, in southern Italy (Fig. 1b), is an important node of the Italian network of the Middle Pleistocene terrestrial tephrostratigraphic archives documenting the peri-Tyrrhenian explosive activity during the 560–490 ka time span (Petrosino et al., 2014b). The Acerno tephra layers were previously analyzed by acquiring major element compositions of glasses by Munno et al. (2001) and Petrosino et al. (2014b). These data, along with $^{40}Ar/^{39}Ar$ geochronological constraints obtained on sanidine crystals, allowed Petrosino et al. (2014b) to attribute the tephra layers to Latium and Campania volcanic sources and to propose preliminary correlations of some of them with known explosive events occurred at Colli Albani and Sabatini volcanic districts (Fig. 1a). During the last decades, investigation of tephra from several marine and continental successions of Central and Southern Italy, as well as from the wider Mediterranean area, evidenced a tephrostratigraphic framework at least partially overlapping the Acerno succession (Fig. 1b). Among these, the Middle Pleistocene lacustrine succession of the intermontane Mercure basin (Southern Italy) hosts 17 tephras, constrained between ~570 and ~440 ka, many of which have been correlated with some from Acerno (Giaccio et al., 2014; Petrosino et al., 2014a). Tephrostratigraphic analyses of three volcanic ash layers in the lacustrine-fluvial sediments core drilled in the intermountain Sulmona basin (Central Italy) allowed for the attribution of the investigated succession to the ~500–410 ka interval (Regattieri et al., 2016). Moreover, in several outcrops and cored sediments of the Sulmona basin, Giaccio et al. (2013b) recognized at least ten ash layers, which span the ~800–450 ka time period. The investigation of the DEEP site sediment record of Lake Ohrid (Albania-North Macedonia), which possibly shares tephra layers with the Acerno, Mercure and Sulmona successions, provides insights into the central Mediterranean explosive volcanic activity during the last 1.36 Ma (Leicher et al., 2016, 2019, 2021). Similarly, in the deep sea sediment core ODP site 964 (Ionian basin) succession, which spans the last 800 ka, one tephra layer was correlated with potential equivalents of the Mercure and Acerno basins (Vakhrameeva et al., 2021). A schematic reconstruction of the entire tephrostratigraphic framework for the Acerno time interval is reported in Fig. 1b.

Recent studies indicate that, in addition to major, minor and trace element compositions commonly used for tephrostratigraphic correlations, isotopic ratios such as $^{87}Sr/^{86}Sr$ and $^{143}Nd/^{144}Nd$ are an additional powerful, integrative tool for identifying the volcanic sources of individual tephra (e.g., Giaccio et al., 2013a, 2014, 2017b; D'Antonio et al., 2016; Petrosino et al., 2019; Monaco et al., 2022a,b). However, the composition (i.e., major, trace elements and radiogenic isotopes) of some proximal and distal deposits from Italian volcanic centers emplaced during the Quaternary remains poorly documented. This deficiency represents one of the limiting factors in tephrostratigraphy. A complete geochemical dataset is still missing also for tephra of the various distal basins. For instance, trace element compositions of the Mercure tephra (Giaccio et al., 2014) and isotopic compositions of the Lake Ohrid and ODP site 964 tephra (Leicher et al., 2016, 2019; Vakhrameeva et al., 2021) have not yet been determined, whereas for the Sulmona basin (Giaccio et al., 2013b; Regattieri et al., 2016) to date only major element compositions have been acquired on a limited number of tephra possibly coeval with the Acerno tephra. The use of uncompleted dataset still affects the outcomes of studies aimed at referring distal tephra from various terrestrial and marine archives to their possible proximal equivalents, as well as making inter-archive correlations.

To identify the volcanic source of tephra layers and enhance the knowledge of activity of Campania and Latium volcanoes in the considered time period, we analyzed trace element contents and Sr–Nd isotopic ratios of the twenty-one tephra layers embedded in the lacustrine sediments of the Acerno basin (Fig. 1c). The newly acquired dataset is compared with existing literature data from sub-coeval explosive activity of Italian volcanoes, documented in both proximal and distal records. Using the published sanidine $^{40}Ar/^{39}Ar$ ages of four tephra layers present in the Acerno sedimentary sequence, together with chronological constraints available for their correlatives, we then developed a Bayesian age-depth model, which results in an improved chronology for the investigated record and, by extension, for the tephrostratigraphic framework of the Central Mediterranean. The age of the basal part of the Acerno succession, formerly at ~560 ka, is here constrained at ~570 ka. Similarly, the topmost part, formerly at ~490 ka, is here constrained at ~470 ka. Moreover, another significant outcome of this study is the development of a standardized procedure utilizing Sr and Nd isotopic ratios as powerful tools for tephrostratigraphic purposes. When combined with major and trace element data and geochronological constraints, the isotopic signature allows strengthening the proximal-distal tephra correlation and provides reliable attributions. This enables us to unambiguously identify the main marker layers within the ~570–470 ka time span. This approach is also advocated for other time intervals, with the goal of establishing a precise tephra framework for the Middle Pleistocene in the Mediterranean region. Such a framework would offer robust chronological constraints for this time period to the broader community of Quaternary scientists.

2. Previous investigations on the Acerno succession

The Acerno basin (Fig. 1b) is a Quaternary Apennine intermountain graben located in the south-western sector of the limestone Picentini Mts., east of the city of Salerno (Campania region). It is a tectonic depression filled by about 120 m of continental sediments, observed in scattered outcrops as described by Capaldi et al. (1988). Russo Ermolli (2000), Munno et al. (2001) and Petrosino et al. (2014b) investigated in detail the succession of a ~100 m deep borehole drilled in the depocenter of the basin (40°49′50″ N - 15°02′44″ E − 650 m a.s.l.). The succession starts with 3 m of alluvial sandy gravels, which are covered by about 60 m of an alternation of laminated lacustrine silts and silty-sands, interbedded with numerous tephra layers (Fig. 1c). Starting from 36 m depth upward, scattered levels of alluvial sandy gravels are interfingered with silty and sandy levels. The twenty-one investigated pyroclastic layers (0.5–20 cm thick), which occur in the lower 60 m of the succession, labeled from A1 to A20, are composed of whitish to dark-gray, dense to well-vesicular, aphyric to porphyritic pumice, scoria and minor lithic fragments and are extensively described by Petrosino et al. (2014b). As explained in Petrosino et al. (2014b), the A18 layer of Munno et al. (2001) has been split into two sublayers (A18a and A18b, each 1-cm thick) with very different major element compositions, since they represent the products of different eruptive events.

Four $^{40}Ar/^{39}Ar$ age determinations carried out on sanidine crystals of

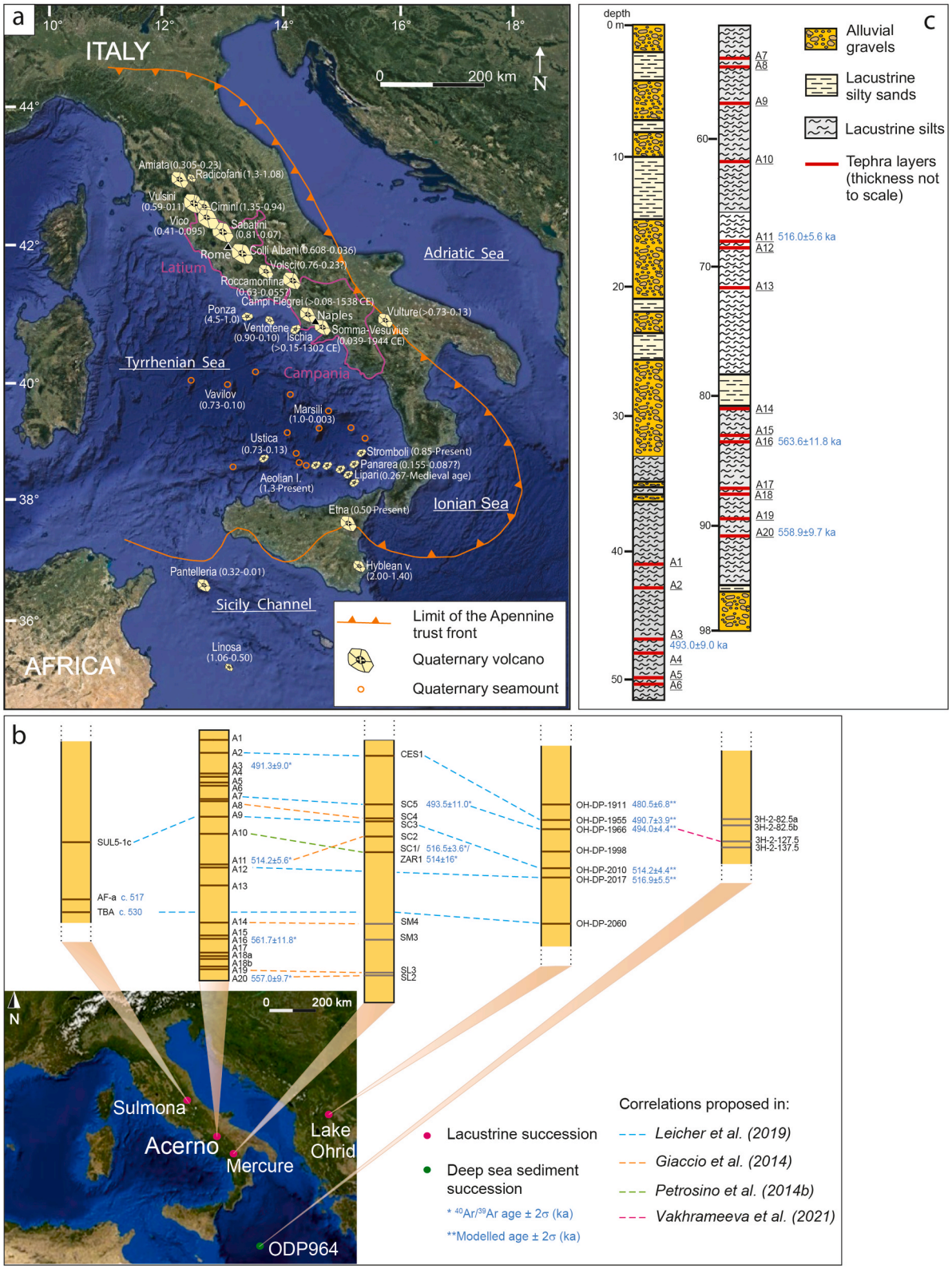

Fig. 1. a) Location of the Italian Quaternary volcanoes with indication of the time interval of activity (Ma, unless differently indicated; modified after Branca et al., 2023); b) location of other archives with tephra emplaced in the same age range of the Acerno tephra; stratigraphic position, age constraints of distal tephra and correlations argued or hypothesized in previous works (Giaccio et al., 2014; Petrosino et al., 2014a, 2014b; Leicher et al., 2016, 2019, 2021; Regattieri et al., 2016; Vakhrameeva et al., 2021) are shown; c) depth and lithology of the Acerno succession with position of the twenty-one tephra from the shallowest (A1) to the deepest (A20) investigated layer and published $^{40}Ar/^{39}Ar$ ages recalculated in this work (see section 3.3). Details on the geological setting are given in Petrosino et al. (2014b).

A3, A11, A16 and A20 volcanic ash layers constrain the deposition of the drilled sediments to the late Middle Pleistocene, and the emplacement of tephra between at least ~560 and 490 ka (Fig. 2; Petrosino et al., 2014b).

These ages are consistent with palynological and tephrostratigraphic analyses revealing that the sedimentation in this lacustrine succession had a maximum duration of 150 kyr and occurred during the Marine Isotope Stage (MIS) 14, 13 and part of 12 (Russo Ermolli, 2000; Munno et al., 2001; Petrosino et al., 2014b). Also, paleomagnetic data on Quaternary intramontane basins in the Picentini mountains confirm that the Acerno sedimentary sequence was emplaced during the Brunhes chron (Porreca and Mattei, 2010).

For each tephra layer, a first preliminary correlation with volcanoes active in Italy during the Middle Pleistocene was hypothesized by Petrosino et al. (2014b), based on major element composition and inferred age of the tephra. The proposed correlations are schematically reported in Fig. 2, alongside with the composition of glasses making up the distal tephra.

2.1. Terminology used with tephra originated from the Campania region

For the purposes of the present paper, we refer to the same volcanic sources of Petrosino et al. (2014b) reported in Fig. 2. However, it is worthwhile to highlight that there is large variety in the nomenclature used in the literature to indicate the source(s) of tephra from the Campania region, particularly for the tephra emplaced before the Campanian Ignimbrite event (CI; 39.85 ± 0.14 ka; Giaccio et al., 2017a; Campi Flegrei). This event produced the equivalent marine marker tephra layer Y-5, which is widely distributed in the Mediterranean and beyond. For instance, Rolandi et al. (2003) introduced the term Campanian Volcanic Zone (CVZ) to indicate the area of Campania where the currently active Ischia, Campi Flegrei and Somma-Vesuvius, as well as the extinct Roccamonfina volcanic districts are located. Insinga et al. (2014), who found at least 9 pre-CI tephra layers in the KC01B deep-sea core (Ionian Sea, Central Mediterranean) ascribable to this area, pointed to their source with the term "Campania Plain". This term refers to the ~3000 km^2 wide graben-like structural depression generated by Pliocene-Quaternary extensional processes in which the active volcanic sources lie. Other authors (e.g., Petrosino et al., 2014b; Leicher et al., 2019) refer to the "CVZ" to indicate tephra layers originated from the ancient stages of volcanic activity in Campania, except Roccamonfina. In other papers, some tephra layers were ascribed to an unspecified "Campanian volcanism" (e.g., Wulf et al., 2012), or to an undefined "Neapolitan volcanic area" (e.g., Giaccio et al., 2017b). Conte et al. (2020) highlighted the chemical differences between the products of the Pontian islands and those of the "Campanian Volcanic Region", referring to the Plio-Pleistocene activity of the area.

For these reasons, a further aim of this work is to establish a coherent use of the terminology associated with the ancient volcanic activity of the Campania region. We propose the "Neapolitan Volcanic Area" as the area which originated the volcanism that preceded the Campanian Ignimbrite event (i.e., older than ~40 ka). The products of this volcanic activity are geochemically similar to those of the currently active Ischia, Campi Flegrei and Somma-Vesuvius volcanic districts, which were not yet identified as such before the CI event. Thus, the Roccamonfina remains a distinct volcanic district that, indeed, produced distal tephra which here (see Results section) are compositionally well distinguished from those of the Neapolitan Volcanic Area.

3. Analytical methods

3.1. Trace element compositions

Trace element compositions have been acquired on the same glass fragments embedded in epoxy resin and polished on which Petrosino et al. (2014b) had determined the major element contents, on individual glass fragments through SEM-EDS, except sample A18a, whose glasses were not suitable for Laser Ablation.

Trace element concentrations were determined by Laser Ablation – Inductively Coupled Plasma – Mass Spectrometry (LA-ICP-MS) at the Department of Physics and Geology, University of Perugia. The instrumentation is made up of a Teledyne/Photon Machine G2 LA device equipped with a two-volume ANU HelEx 2 cell coupled with a Thermo Scientific quadrupole-based iCAP Q ICP-MS device. The operating conditions were optimized before each analytical session by continuous ablation of international reference standard NIST SRM 612 in order to provide maximum signal intensity and stability for the ions of interest and suppressing the formation of oxides (ThO^+/Th^+ below 0.5%). The U/Th ratio was also monitored, and the value maintained close to 1. The stability of the system was evaluated based on ^{139}La, ^{208}Pb, ^{232}Th and ^{238}U isotopes by a short-term stability test. It consisted of five acquisitions (1 min each) on a linear scan of the NIST SRM 612. The glass fragments were analyzed by using a circular laser beam with a diameter of 20 μm, a frequency of 10 Hz and a laser density on the sample surface of 3.5 J cm^{-2}. The NIST SRM 610, NIST SRM 612, USGS BHVO-2G, USGS GSD-2G reference materials was used for the calibration and ^{29}Si as an internal standard (Paul et al., 2023). The USGS BCR-2G reference material was analyzed as unknown in order to provide a quality control. Under these operating conditions, precision and accuracy were better than 10% for all elements. Further details on the instrumentation are reported in Petrelli et al. (2016). The trace elements contents of the Acerno tephra are reported in Supplementary Material S1.

3.2. Sr–Nd isotopic compositions

$^{87}Sr/^{86}Sr$ and $^{143}Nd/^{144}Nd$ isotopic ratios have been measured either on glass fragments and/or mineral fractions (feldspar, pyroxene) or on whole tephra (hereafter, bulk rock) due to the paucity of available material for some samples of the cored succession (Fig. 2). Moreover, the $^{143}Nd/^{144}Nd$ isotopic ratios have been also acquired on glass fragments isolated from five tephra layers from the Mercure basin described by Giaccio et al. (2014), in order to complete the isotopic characterization of these tephra possibly equivalent to Acerno layers (in Supplementary Material S2 detailed information on the succession and on the available data are reported).

From each tephra layer of the cored succession glass fragments, and, when possible, feldspar and/or pyroxene grains, have been hand-picked from grain size classes comprised between 1 mm and 250 μm. Where available, a few larger juvenile clasts have been gently crushed to fine-size (<1 mm) grains through a jaw crusher. When the tephra was finer than 250 μm, the bulk rock has been analyzed. The hand-picked fragments and minerals have been washed in an ultrasonic bath to remove encrusted clay patinas and then dried at 60 °C for 24 h. The different fractions have been observed under a binocular microscope in order to further remove altered material before chemical processing. A1, A14 and A20 grains resulted deeply clay-encrusted after pretreatment and, as a consequence, no isotopic measurement was carried out on their bulk rock or glass fragments. The Sr isotopic ratios have been measured on feldspar crystals of these layers, except for A1 tephra due to the paucity of crystals (Petrosino et al., 2014b).

The whole set of Sr–Nd isotopic data from Acerno basin samples has been determined by thermal ionization mass spectrometry (TIMS) at the University of Naples (Dipartimento di Scienze della Terra, dell'Ambiente e delle Risorse), using a Triton Plus® (Thermo Scientific) solid-source multicollector mass spectrometer. The chemical treatment of the samples was carried out in a laminar flow hood equipped with two class H13 (EN 1822) HEPA filters, located in an ISO 6 clean room at the University of Naples. Before chemical dissolution, glassy fragments, bulk rock, feldspar and pyroxene grains have been acid leached three times to reduce alteration effects. Leaching has been carried out each time by placing the beakers containing samples and ca. 1 mL of 6M HCl on a hot plate for 10 min. After the leaching steps, samples have been rinsed with

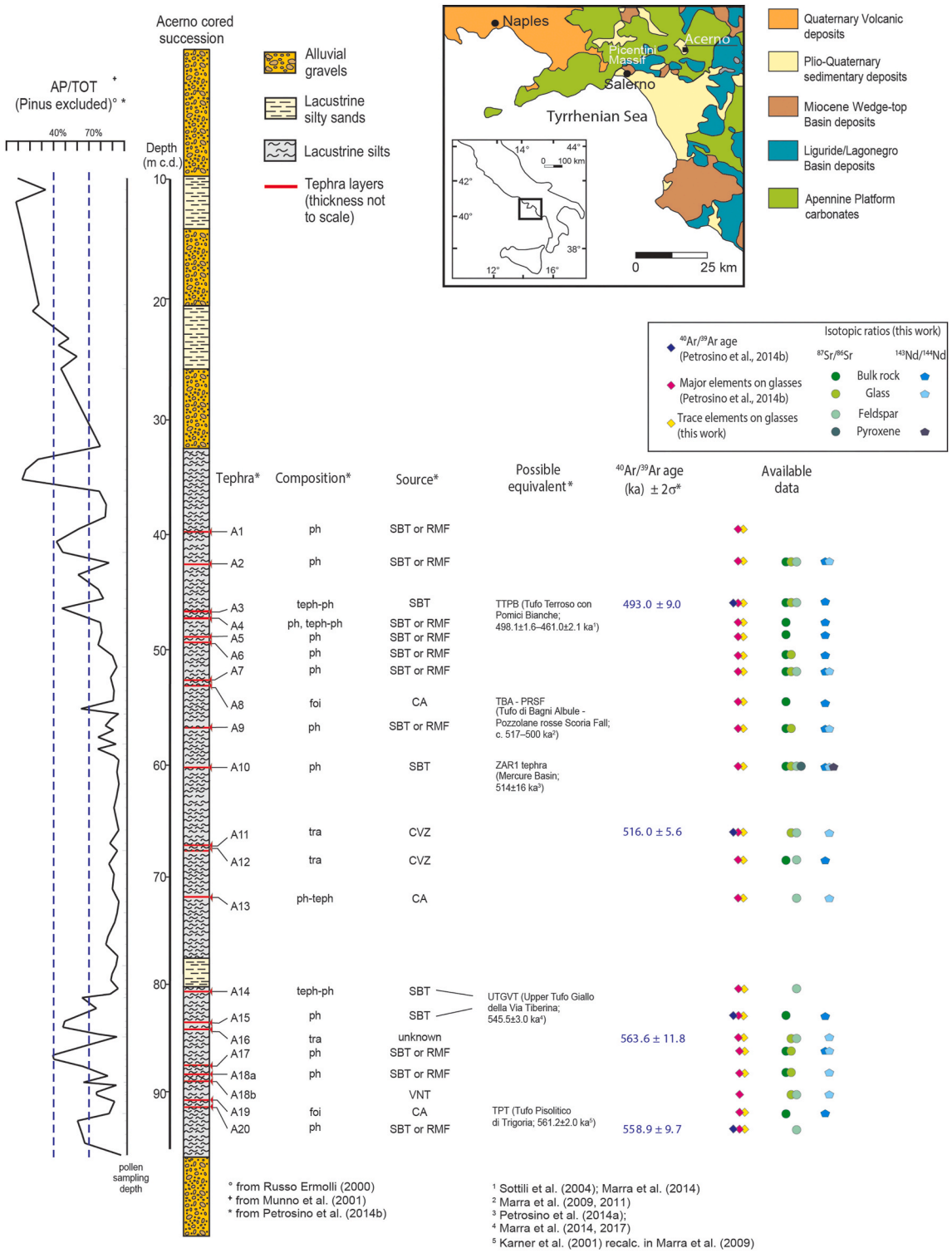

Fig. 2. Acerno cored succession summarizing the previous knowledge (Russo Ermolli, 2000; Munno et al., 2001; Petrosino et al., 2014b) and showing the type of the already available (Petrosino et al., 2014b) and newly acquired geochemical data. The insert in the top right corner shows a schematic geological map with the location of the Acerno basin (modified from Petrosino et al., 2014b). The reported $^{40}Ar/^{39}Ar$ ages for the Acerno tephra have been recalculated as described in section 3.3. Possible equivalent refers to known eruptive events and to tephra from other distal archives; ph: phonolite; ph-teph: phono-tephrite; foi: foidite; teph-ph: tephri-phonolite; tra-ph: trachy-phonolite; tra: trachyte; SBT: Sabatini; RMF: Roccamonfina; CA: Colli Albani, CVZ: Campanian Volcanic Zone (Rolandi et al., 2003); VNT: Ventotene. On the left: AP (arboreal pollen) values over 70% indicate densely forested environments of typical interglacial conditions; values below 40% indicate open environments of typical glacial conditions; values between 70 and 40% indicate patchy landscapes with a mosaic of forested areas and open spaces (Favre et al., 2008), typical of transitional climatic phases.

Milli-Q® deionized water. Following leaching, the above-mentioned fractions have been dissolved with high-purity HF–HNO_3–HCl mixtures. Sr and Nd have been separated from the matrix through conventional ion-exchange chromatographic procedures, described in detail in Arienzo et al. (2013).

Chemical dissolution and Nd isotopic ratios from Mercure basin samples have been performed at the Radiogenic Isotope Laboratory of the Istituto Nazionale di Geofisica e Vulcanologia, Osservatorio Vesuviano. Nd isotopic ratios have been measured by TIMS, using a Triton XT Plus® (Thermo Scientific) solid-source multicollector mass spectrometer.

The blank for Sr was about 100 pg during the period of chemistry processing, negligible considering the average Sr content of the samples; no determinations for Nd blanks was needed given the cleanliness of the laboratories. Measured $^{87}Sr/^{86}Sr$ and $^{143}Nd/^{144}Nd$ ratios have been normalized for within-run isotopic fractionation to $^{88}Sr/^{86}Sr = 8.375209$ and $^{146}Nd/^{144}Nd = 0.7219$, respectively, using an exponential law for correction. During collection of isotopic data, replicate analyses of NIST-SRM 987 and JNdi-1 international reference standards have been performed to check for external reproducibility. During the period of analysis, the mean measured value (Goldstein et al., 2003) of $^{87}Sr/^{86}Sr$ for NIST-SRM 987 was 0.710234 ± 0.000013 (2σ, where σ is the standard deviation of the values; n = 48); that of $^{143}Nd/^{144}Nd$ for JNdi-1 was 0.512095 ± 0.000006 (2σ, n = 31) at the University of Naples and that of $^{143}Nd/^{144}Nd$ for JNdi-1 was 0.512105 ± 0.000007 (2σ, n = 20) at Osservatorio Vesuviano. Sr and Nd isotopic ratios of the samples have been normalized to the recommended values of NIST-SRM 987 and JNdi-1 ($^{87}Sr/^{86}Sr = 0.710248$; $^{143}Nd/^{144}Nd = 0.512107$; Zhang and Hu, 2020), respectively.

3.3. Age-depth model

Age-depth modelling was performed using the software package Bacon v. 3.1.1 (Blaauw and Christen, 2011) within the open-source statistical environment R (R Core Team, 2022). The model comprises the portion of the core between 33.0 m and 95.0 m, corresponding to the part of the Acerno succession in which the twenty-one tephra layers have been found (Fig. 1c). The model is based on the four ages obtained from direct $^{40}Ar/^{39}Ar$ dating of the Acerno tephra in Petrosino et al. (2014b) and five $^{40}Ar/^{39}Ar$ ages on correlated tephra layers as discussed below (see section 5; Supplementary Material S2). In addition, the ages of six tie points were transferred from the Lake Ohrid chronology

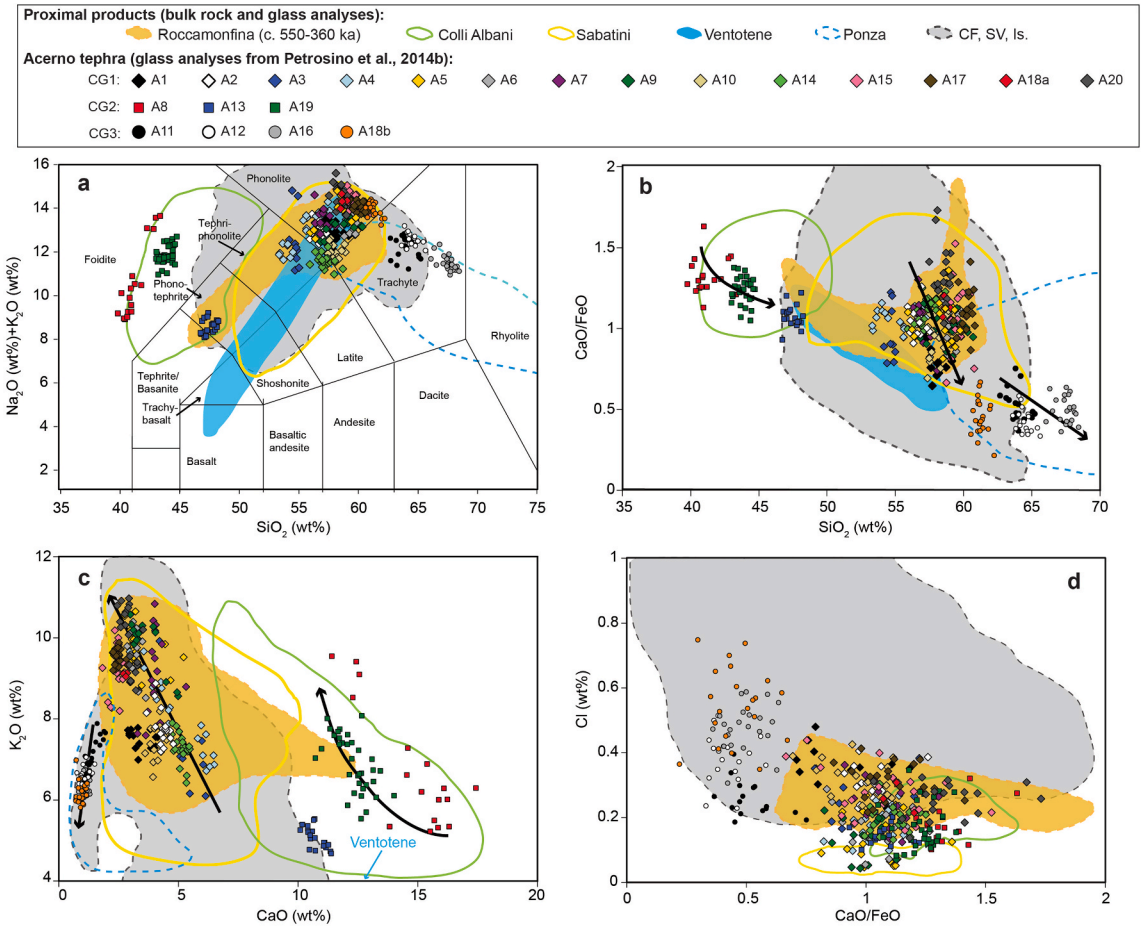

Fig. 3. a) Total Alkali versus Silica (TAS; Le Maitre, 2002) diagram, b) CaO/FeO vs SiO_2 (wt%) diagram, c) K_2O (wt%) vs CaO (wt%) diagram and d) Cl (wt%) vs CaO/FeO diagram for the investigated tephra layers (data from Petrosino et al., 2014b); black arrows indicate the different evolution trends of the three CGs; CF: Campi Flegrei, SV: Somma-Vesuvius, Is: Ischia island. Compositional fields of the proximal products from the volcanic complexes are made up by interpolation of all data points relative to bulk rocks and glass data from literature, if available; the Supplementary Material S3 shows the same diagrams with the single analytical points. Literature data for Colli Albani are from Gaeta et al. (2006, 2011, 2016, 2021), Marra et al. (2009, 2011) and Giaccio et al. (2013a); for Sabatini from Sottili et al. (2004), Masotta et al. (2010), Marra et al. (2011, 2014, 2017), Palladino et al. (2014) and Di Rita and Sottili (2019); for Roccamonfina volcano from Rouchon et al. (2008), Conticelli et al. (2009); for Pontian islands from D'Antonio and Di Girolamo (1994), D'Antonio et al. (1999a), Conte and Dolfi (2002), Conticelli et al. (2002), Cadoux et al. (2005, 2007), Conte et al. (2016); for Campi Flegrei, Somma-Vesuvius and Ischia island from Melluso et al. (1995), de Vita et al. (1999), Andronico and Cioni (2002), D'Oriano et al. (2005), Santacroce et al. (2008), Fedele et al. (2009), Smith et al. (2011), Fourmentraux et al. (2012), Tomlinson et al. (2012, 2014), Arienzo et al. (2015, 2016) and Forni et al. (2016, 2018).

(Wagner et al., 2019) based on comparison between the AP-*Pinus* curve of the Acerno succession (Fig. 2) and that of Lake Ohrid (Donders et al., 2021), as discussed in section 5.2. All $^{40}Ar/^{39}Ar$ ages were recalculated using the software ArAR with a given decay constant of Renne et al. (2011) and an age for ACs-2 (1.1891 Ma; Niespolo et al., 2017) and Fish Canyon sanidine ages of 28.294 Ma (Renne et al., 2011). Based on the evaluation of all chronological tie points, a significant lower sedimentation rate was identified below ~80.4 m (0.07 vs. 0.03 cm/a), which was considered within the age model via a boundary function. The modelled interval of the succession was set into 20 cm vertical sections for modelling individual accumulation rates at a 95% confidence interval, which provide the basis for the age-depth model.

4. Results

4.1. Compositional groups (CG) of the Acerno tephra based on major element concentration

Published major element compositions of glasses extracted from the Acerno tephra layers are plotted in Fig. 3 (Petrosino et al., 2014b). They cluster into three groups, hereafter referred to as Compositional Groups (CGs).

CG1 comprises most of the Acerno tephra layers (A1, A2, A3, A4, A5, A6, A7, A9, A10, A14, A15, A17, A18a and A20). These tephra layers have a phonolitic to tephri–phonolitic glass composition (Figs. 2 and 3a) and show variable amounts of K-feldspar, leucite, biotite and clinopyroxene (Petrosino et al., 2014b). CG2 comprises samples A8 and A19, which have a foiditic glass composition and sample A13, which is phono-tephritic in composition (Figs. 2 and 3a). These three samples contain variable amounts of leucite and clinopyroxene (Petrosino et al., 2014b). CG3 comprises the trachytic samples A11, A12 and A16 and sample A18b that straddles the boundary between the trachyte and phonolite compositional fields in the TAS diagram (Figs. 2 and 3a). These four samples are characterized by a K-feldspar, biotite and clinopyroxene mineral assemblage (Petrosino et al., 2014b). Glass, if available, and bulk rock compositions of proximal volcanic products belonging to the Campi Flegrei, Somma-Vesuvius, Ischia island, Roccamonfina, Pontian islands (Ponza and Ventotene islands), Sabatini, and Colli Albani districts are represented by colored fields in Fig. 3 for comparison. Tephra from CG1 show compositions pertaining to both the Sabatini and Roccamonfina volcanoes, tephra from CG2 display compositions typical of the Colli Albani district, and tephra from CG3 are characterized by major element contents similar to the products erupted from the Pontian islands, Campi Flegrei, Somma-Vesuvius and Ischia island (see also Petrosino et al., 2014b). However, in the light of the newly acquired trace element and isotopic compositions, some of these correlations have been strengthened and/or revised, as discussed in section 5.

4.2. Trace elements

Trace element contents of glass fraction of Acerno tephra layers normalized to primitive mantle (Fig. 4) overall show the typical patterns of the Italian subduction related magmas (e.g., Peccerillo, 2017 and references therein).

Most tephra show enrichment in some strongly incompatible elements such as Rb, Ba, K, Sr (large-ion lithophile elements, LILE) and Pb, as well as in light rare-earth elements, and depletion in others, such as Nb, Ta, Ti (high-field strength elements, HFSE). The A15, A17, A20 and CG3 tephra have significantly low Ba and Sr contents. The HFSE content is quite similar for the three CGs of Acerno tephra previously defined through the glass major element composition (Fig. 3). In fact, Nb content of CG1 is in the range 18–69 ppm and that of CG2 is in the range 23–69 ppm. Glass from CG3 has the highest Nb contents ranging from 34 to 101 ppm (Fig. 5a).

Zr content ranges from 247 to 984 ppm in CG1, from 332 to 729 ppm in CG2 and from 452 to 1300 ppm in CG3. Small variations in the ranges of Hf and Ta among the three CGs are also present (Supplementary Material S1).

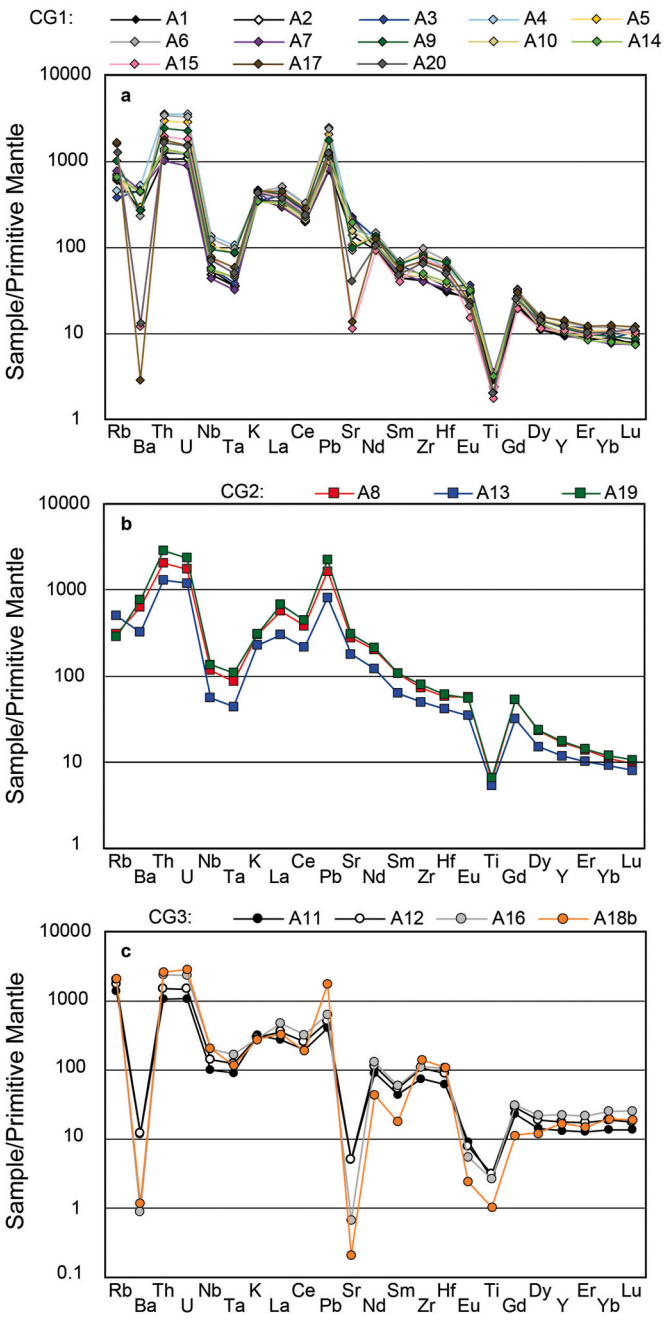

Fig. 4. Primitive mantle normalized trace elements distribution of the Acerno tephra layers (normalization values from Lyubetskaya and Korenaga, 2007).

Overall LILE contents of CGs 1 and 2 show similar ranges and are different from those of CG3. For example, Rb and Sr contents of CG1 are in the range 116–794 ppm and 92–4810 ppm, respectively. In CG2, they vary from 66 to 381 ppm and from 2300 to 5960 ppm, respectively. In CG3, Rb and Sr vary in the range 530–1068 ppm and 1–162 ppm, respectively (Fig. 5; Supplementary Material S1). The CG3 tephra also show significantly low Eu contents. Some differences among the three CGs are detected also in compatible element contents, such as Ni and V. Ni content ranges from 1 to 20 ppm in CG1, from 3 to 68 ppm in CG2 and from 3 to 29 ppm in CG3. V content ranges between 37 and 206 ppm in CG1, 264 and 461 ppm in CG2, and 12 and 52 ppm in CG3 (Fig. 5c; Supplementary Material S1).

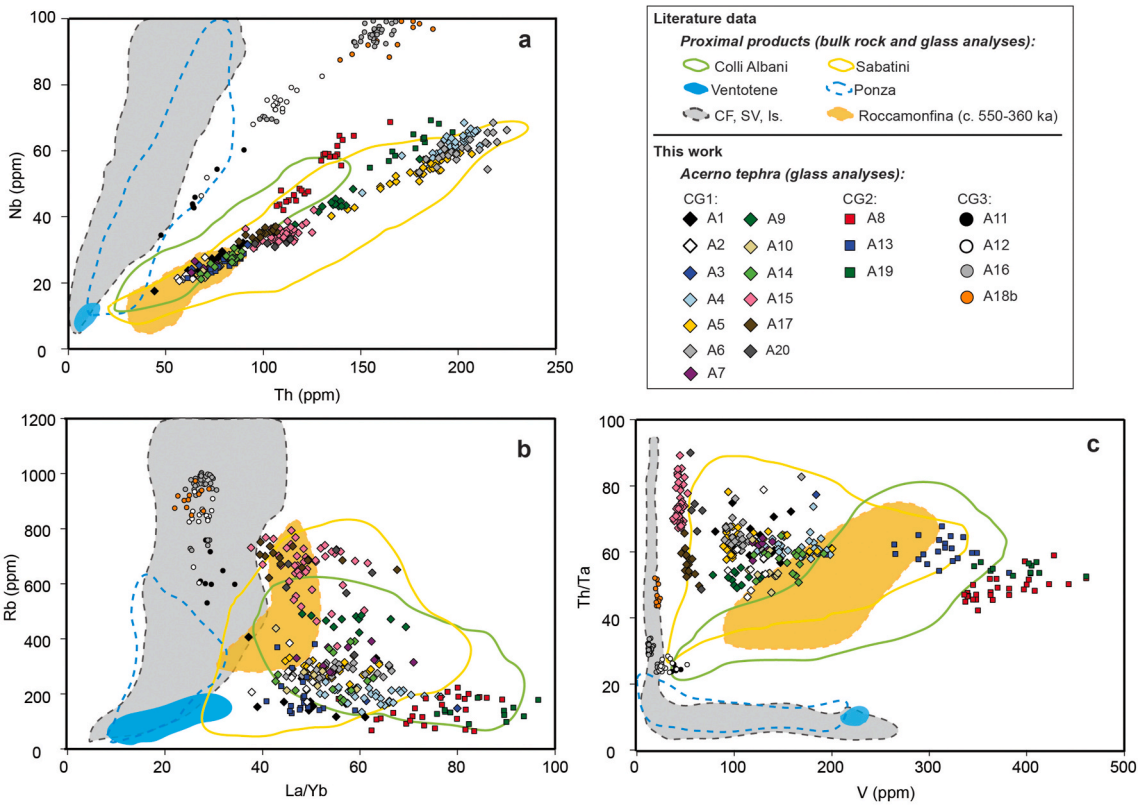

Fig. 5. a) Nb (ppm) vs Th (ppm) diagram, b) Rb (ppm) vs La/Yb diagram and c) Th/Ta vs V (ppm) diagram for the investigated tephra layers. CF: Campi Flegrei, SV: Somma-Vesuvius, Is: Ischia island. Compositional fields of the volcanic complexes are made up by interpolation of all data points relative to bulk rocks and glass data from literature, if available; the Supplementary Material S4 shows the same diagrams with the single analytical points. Literature data for Colli Albani are from Giordano et al. (2006), Boari et al. (2009), Gaeta et al. (2011, 2021) and Marra et al. (2011); for Sabatini from Conticelli et al. (1997, 2007), Gasperini et al. (2002), Sottili et al. (2004), Marra et al. (2011, 2014, 2017) and Monaco et al. (2022a); for Roccamonfina volcano from Giannetti and Ellam (1994), Di Girolamo et al. (1991), Rouchon et al. (2008), Conticelli et al. (2009); for Pontian islands from D'Antonio and Di Girolamo (1994), D'Antonio et al. (1999a), Conte and Dolfi (2002), Conticelli et al. (2002), Cadoux et al. (2005, 2007), Conte et al. (2016); for Campi Flegrei, Somma-Vesuvius and Ischia island from Hawkesworth and Vollmer (1979), Joron et al. (1987), Poli et al. (1987), Crisci et al. (1989), Beccaluva et al. (1991), Civetta et al. (1991, 1997), Civetta and Santacroce (1992), Orsi et al. (1992, 1995), Caprarelli et al. (1993), Santacroce et al. (1993), Villemant et al. (1993), Cioni et al. (1995), Di Girolamo et al. (1995), D'Antonio et al. (1999b), Ayuso et al. (1998), de Vita et al. (1999), Pappalardo et al. (1999, 2002, 2008), Conticelli et al. (2002), Lustrino et al. (2002), D'Oriano et al. (2005), Paone (2006), Piochi et al. (2006), Di Renzo et al. (2007), Aulinas et al. (2008), Pabst et al. (2008), Arienzo et al. (2009), Marturano et al. (2009), Tonarini et al. (2009), Tomlinson et al. (2012, 2014, 2015) and Brown et al. (2014). (For interpretation of the references to color in this figure legend, the reader is referred to the Web version of this article.)

In summary, trace element data support the discrimination of the three CGs selected based on major element compositions of the Acerno tephra (Fig. 3). Incompatible elements, such as HFSE and LILE, and ratios among different elements such as Nb (ppm) vs Th (ppm) variation diagram, Rb (ppm) vs La/Yb and the Th/Ta vs V (ppm) allow distinguishing different trends among these CGs (Fig. 5; Supplementary Material S4 shows single analytical points used for comparison). In fact, the comparison with the composition of proximal products shows that tephra of CG1 follow the trend defined by products of the Sabatini district (yellow field in Fig. 5a) characterized by relatively low Nb/Th ratios. Tephra of CG3 show a trend observed for Pontian islands, Campi Flegrei, Somma-Vesuvius and Ischia island volcanic products (gray and light blue fields in Fig. 5a), characterized by relatively high Nb/Th ratios. The tephra associated to CG2 plot in between CG1 and CG3, following the trend of Colli Albani products (green field in Fig. 5a).

4.3. Sr–Nd isotopic compositions

The Sr and Nd isotopic ratios of the Acerno and Mercure tephra are reported in Table 1.

Some measurements have been repeated and, in this case, we report, in Table 1, the average of two values weighted in proportion to their error (Supplementary Material S1).

According to Petrosino et al. (2014b), the Acerno tephra show, overall, a low amount of loose crystals with respect to the glass and lithic fractions. Also, there is a prevalence of felsic (leucite, feldspar) over mafic phases. The Sr and Nd isotopic values are consistent across the various analyzed phases (bulk rocks, glass, feldspar and pyroxene) of each sample, except for sample A18b. Overall, Sr isotopic ratios cover a wide range, varying between 0.70819, the least radiogenic value measured on feldspar phenocrysts of the A16 tephra and 0.71121, the most radiogenic value measured on A19 bulk rock (Table 1). The Nd isotopic ratios, on the other hand, vary between 0.51210, for the A4 bulk rock and 0.51233, for the A15 bulk rock.

The $^{87}Sr/^{86}Sr$ and $^{143}Nd/^{144}Nd$ isotopic ratios of glasses, bulk rock and minerals of CG1 range from 0.70909 to 0.71115 and from 0.51210 to 0.51220, respectively. The Sr isotopic ratios measured in bulk rock and glass of CG2 are in the range 0.71004–0.71122, whereas the Nd isotopic ratios are in the range 0.51211–0.51213 (Fig. 6; Table 1). Glasses, bulk rock and feldspars of CG3 mostly show lower $^{87}Sr/^{86}Sr$ values and notably higher $^{143}Nd/^{144}Nd$ values, with respect to those of CG1 and CG2: the Sr isotopic ratios vary between 0.70819 and 0.70970, whereas the Nd isotopic ratios range between 0.51217 and 0.51233 (Fig. 6; Table 1).

Table 1
$^{87}Sr/^{86}Sr$ and $^{143}Nd/^{144}Nd$ of bulk rock, feldspar, pyroxene and glass fractions of the Acerno and Mercure basins tephra.

Sample	Analyzed material	$^{87}Sr/^{86}Sr$	±2 s.e.	$^{143}Nd/^{144}Nd$	±2 s.e.
A2	Bulk rock	0.709260	±0.000007	0.512179	±0.000004
	Feldspar	0.709088	±0.000007		
	Glass	0.709105	±0.000007	0.512200[a]	±0.000008
A3	Bulk rock	0.709449[a]	±0.000004[a]	0.512174	±0.000005
	Feldspar	0.709862	±0.000007		
	Glass	0.709593	±0.000006		
A4	Bulk rock	0.710994	±0.000006	0.512100[a]	±0.000004
A5	Bulk rock	0.710938[a]	±0.000005[a]	0.512106	±0.000004
A6	Bulk rock	0.711105	±0.000008	0.512102	±0.000005
	Glass	0.711040	±0.000006		
A7	Bulk rock	0.709548	±0.000007	0.512162	±0.000005
	Feldspar	0.709427	±0.000007		
	Glass	0.709512	±0.000007	0.512164	±0.000013
A8	Bulk rock	0.710593[a]	±0.000005[a]	0.512114	±0.000005
A9	Bulk rock	0.711110	±0.000007	0.512105	±0.000004
	Glass	0.711149	±0.000006	0.512106	±0.000005
A10	Bulk rock	0.709716	±0.000007	0.512143	±0.000005
	Feldspar	0.709512	±0.000006		
	Pyroxene	0.709573	±0.000006	0.512162	±0.000005
	Glass	0.709566	±0.000006	0.512156	±0.000005
A11	Feldspar	0.708328	±0.000006		
	Glass	0.708575	±0.000007	0.512331	±0.000004
A12	Bulk rock	0.708907	±0.000006	0.512332	±0.000005
	Feldspar	0.708369	±0.000005		
A13	Glass	0.710041	±0.000006	0.512129	±0.000006
A14	Feldspar	0.709941	±0.000007		
A15	Bulk rock	0.710068[a]	±0.000006[a]	0.512128	±0.000005
A16	Feldspar	0.708194	±0.000006		
	Glass	0.709700	±0.000006	0.512308	±0.000004
A17	Bulk rock	0.709714	±0.000007	0.512161	±0.000004
	Glass	0.709778	±0.000006	0.512159	±0.000005
A18a	Bulk rock	0.709705[a]	±0.000005[a]		
	Glass	0.709769	±0.000006	0.512160	±0.000007
A18b	Feldspar	0.709049	±0.000007	0.512232	±0.000020
	Glass	0.709592	±0.000007	0.512169[a]	±0.000005[a]
A19	Bulk rock	0.711215	±0.000006	0.512120	±0.000005
A20	Feldspar	0.709960[a]	±0.000006[a]		
SM1[b]	Glass	0.710020[c]	±0.000007	0.512134[d]	±0.000006
SC1[b]	Glass	0.709658[c]	±0.000007	0.512125[d]	±0.000006
SL3 bis[b]	Glass	0.711013[c]	±0.000007	0.512101[d]	±0.000006
SL1[b]	Glass	0.709956[c]	±0.000007	0.512133[d]	±0.000007
SL2[b]	Glass	0.709993[c]	±0.000007	0.512135[d]	±0.000006

Reported values are corrected for those of the respective international standards (see text for detail).
s.e. = standard error on each measurement.
[a] Weighted average value of two measurements (the single measurements are in Supplementary Material S1).
[b] Tephra layers from Mercure Basin.
[c] From Giaccio et al. (2014).
[d] This work.

5. Discussion

5.1. Identifying volcanic sources and potential equivalents

We compared the major-, trace-elements and the Sr–Nd isotopic compositions of the Acerno tephra with those of glasses and bulk rocks of proximal and distal products belonging to volcanic districts experiencing explosive activity during the time interval of the deposition of the Acerno tephra (~570–470 ka). First of all, we can exclude some sources, such as Aeolian Islands and Vulture volcanic centers, based on the notable chemical and isotopic differences of their erupted products with respect to those of the Acerno tephra. The products of the Aeolian Islands belong to calc-alkaline suites and are hence very different from the alkaline compositions of the Acerno tephra. Also, the isotopic signature of the Vulture volcanic products ($^{87}Sr/^{86}Sr$ = 0.7071–0.7043; $^{143}Nd/^{144}Nd$ = 0.5130–5125), whose age partly overlaps the Acerno succession, is totally different from that of the investigated tephra (e.g., Peccerillo, 2017; Branca et al., 2023 and references therein). Hence, we consider Latium and Campania volcanoes of the Italian peri-Tyrrhenian margin. In particular, for the Roccamonfina, Sabatini and Colli Albani districts we took into account compositional data, including Sr and Nd isotopic compositions of mineral phases, of proximal products whose age is in the same range of the Acerno tephra.

For the Pontian islands, Campi Flegrei, Somma-Vesuvius and the Ischia island, we considered the chemical and isotopic compositions of glass and bulk rock available in literature for proximal products of different ages. This was prompted by the scarcity of information on the eruptive history and chemistry of the products of these volcanoes during the MIS 14–12. We therefore refer to Campi Flegrei, Somma-Vesuvius and Ischia island, identified as presently known, for comparisons based on the chemical and isotopic signature of their products. However, for the attribution of Acerno tephra emplaced during the pre-CI activity, we turn to the Neapolitan Volcanic Area. Unfortunately, geochemical datasets of glass composition of near-vent products for some Italian Quaternary volcanic districts are still limited or almost completely lacking (e.g., for Roccamonfina). Moreover, we also considered chemical and isotopic compositions of distal tephra from the Mediterranean area deposited in the same age range as the Acerno tephra (Fig. 1b; Giaccio et al., 2013b, 2014; Petrosino et al., 2014a; Leicher et al., 2019, 2021; Vakhrameeva et al., 2021).

The Sr and Nd isotopic ratios reveal to be a powerful tool to assess correlations. The variation of both isotopic ratios detected in the Acerno samples is beyond the analytical uncertainty (section 3.2) and cannot be an effect of radioactive decay, given the relatively young age (less than 1 Ma) of the tephra and their relatively low Rb content. Therefore, the $^{87}Sr/^{86}Sr$ and $^{143}Nd/^{144}Nd$ values reflect magma source features and can be useful for discriminating tephra from different volcanic centers (e.g., Giaccio et al., 2013a, 2014, 2017b; D'Antonio et al., 2016; Petrosino et al., 2019; Monaco et al., 2022a,b).

5.1.1. CG1 tephra

A1, A2, A3, A4, A5, A6, A7, A9, A10, A14, A15, A17, A18a and A20 – The phonolitic to tephri–phonolitic CG1 tephra are characterized by major element compositions fully matching those of the proximal volcanic products of Sabatini, Roccamonfina and, partially, Campi Flegrei, Somma-Vesuvius and Ischia island (Fig. 3). Nevertheless, their trace element compositions clearly allow distinguishing the CG1 tephra from the products of Campi Flegrei, Somma-Vesuvius and Ischia island (gray field in Fig. 5). Indeed, in the Nb (ppm) vs Th (ppm) diagram, these samples have relatively low Nb/Th ratios and follow the trend of the Sabatini and Roccamonfina products, with respect to all the other Acerno layers (yellow and orange fields in Fig. 5a).

These samples also show some differences in the major and trace element contents. For example, A3 and A4 glass composition shows a lower differentiation degree with respect to the other CG1 tephra. Indeed, these two samples plot in the tephri-phonolite field of the TAS diagram (Fig. 3a) and are characterized by relatively lower SiO_2 and Rb contents, and higher CaO, Sr and V contents compared with those of the other CG1 tephra (Figs. 3 and 5; Supplementary Material S1). On the other hand, A15, A17 and A20 tephra are characterized by a more evolved glass composition showing relatively higher SiO_2, Na_2O, K_2O and Rb, and lower CaO, Ba, Sr and V contents with respect to those of other CG1 tephra, which are mostly phonolitic (Figs. 3 and 5; Supplementary Material S1). Also, these three samples differ for having notable Ba and Sr negative peaks in the primitive mantle normalized diagram, likely related to fractionation of alkali-feldspar, with respect to those of the other CG1 tephra (Fig. 4).

All the CG1 tephra layers fall in the major and trace element compositional fields of the Sabatini and the ancient Roccamonfina products, pertaining to the Roccamonfina Synthem of De Rita and Giordano (1996). Synthems are used to rank stratigraphic units and are defined as unconformity-bounded stratigraphical units featured by

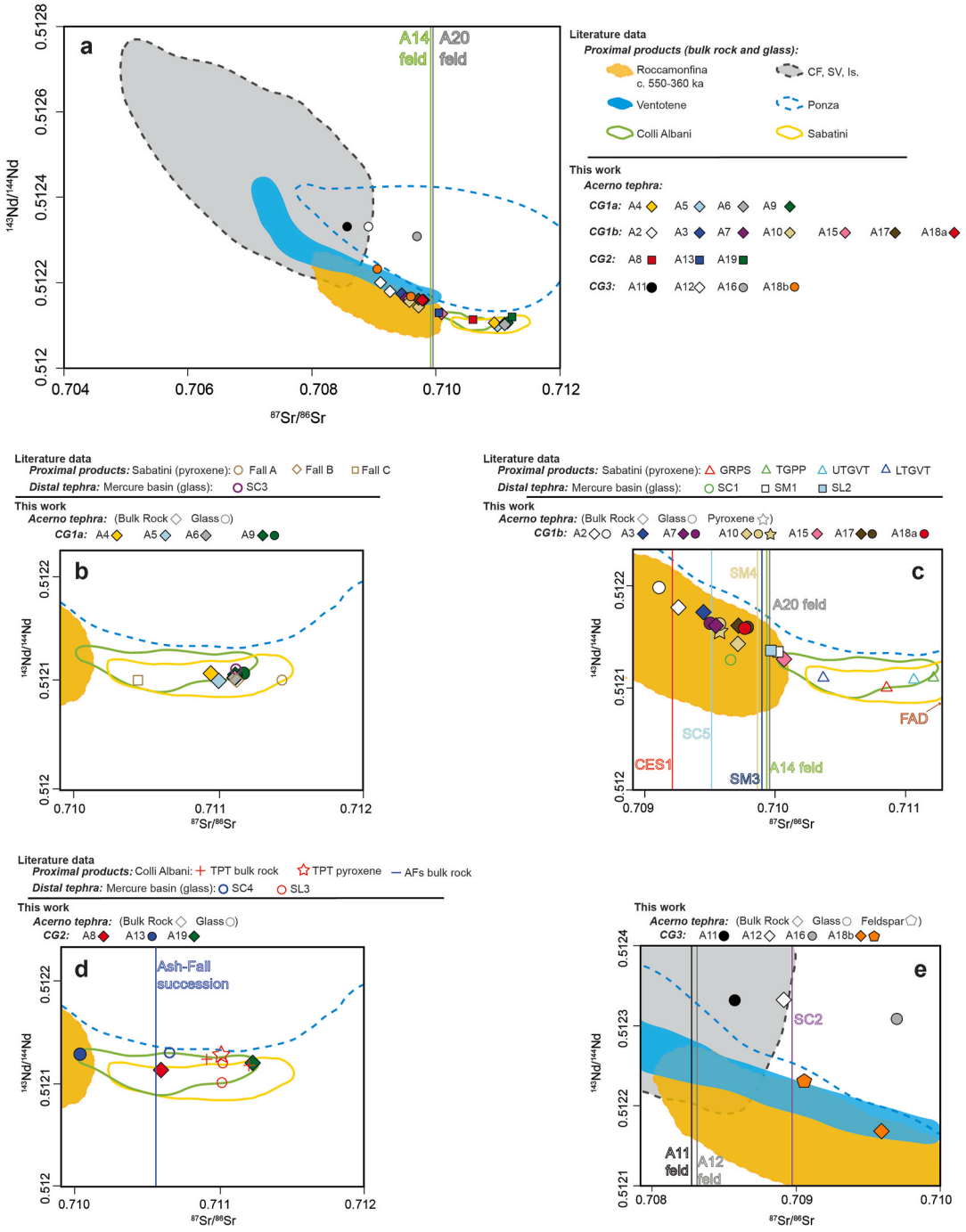

Fig. 6. a) $^{143}Nd/^{144}Nd$ vs $^{87}Sr/^{86}Sr$ diagram for the analyzed samples. The analytical uncertainty of the isotopic ratio values (2s.e.) is within the symbol. CF: Campi Flegrei, SV: Somma-Vesuvius, Is: Ischia island. Literature data for Colli Albani are from Boari et al. (2009), Giaccio et al. (2013a) and Gaeta et al. (2016); for Sabatini from Sottili et al. (2019); for Roccamonfina volcano from Conticelli et al. (2009); for Pontian islands from Barberi et al. (1969), Turi et al. (1991), D'Antonio and Di Girolamo (1994), D'Antonio et al. (1999a), Conte and Dolfi (2002), Cadoux et al. (2005, 2007) and Conte et al. (2016); for Campi Flegrei, Somma-Vesuvius and Ischia island from Hawkesworth and Vollmer (1979), Cortini and Hermes (1981), Civetta et al. (1991, 1997), Turi et al. (1991), Orsi et al. (1992, 1995), Belkin et al. (1993), Caprarelli et al. (1993), Santacroce et al. (1993, 2008), Di Girolamo et al. (1995), D'Antonio et al. (1996, 1999b, 2007, 2013), Ayuso et al. (1998), de Vita et al. (1999), Pappalardo et al. (1999, 2002), Piochi et al. (1999, 2006), Somma et al. (2001), Conticelli et al. (2002), Martelli et al. (2004), Slejko et al. (2004), Tonarini et al. (2004, 2009), Paone (2006), Di Renzo et al. (2007, 2011, 2022), Aulinas et al. (2008), Avanzinelli et al. (2008, 2018), Pabst et al. (2008), Arienzo et al. (2009, 2011, 2015, 2016), Di Vito et al. (2011), Brown et al. (2014), Koornneef et al. (2015), Casalini et al. (2017), Iovine et al. (2017), Sparice et al. (2017), Forni et al. (2018), Voloschina et al. (2018), Buono et al. (2020), Di Salvo et al. (2020), Pelullo et al. (2020); b-e) details of Fig. 6a showing the comparison between the Acerno samples and i) the Mercure basin tephra and ii) proximal products belonging to specific Sabatini and Colli Albani eruptive events; the meaning of the CG1a and CG1b grouping is given in section 5.1.1; for abbreviation see the text; literature data for FAD, LTGVT, UTGVT, TGPP, GRPS, Fall A, Fall B and Fall C from Sottili et al. (2019); for Ash-Fall succession from Giaccio et al. (2013a) and for TPT from Giaccio et al. (2013a) and Gaeta et al. (2016); for Mercure basin tephra, the Sr and Nd isotopic ratios are from Giaccio et al. (2014) and this work (Supplementary Material S2); vertical lines indicate samples for which only the $^{87}Sr/^{86}Sr$ ratios have been measured. (For interpretation of the references to color in this figure legend, the reader is referred to the Web version of this article.)

simple and broad criteria of applicability (see Salvador, 1994). The Roccamonfina Synthem includes the deposits older than 358 ka, the age of Brown Leucitic Tuff which is the first deposit pertaining to the younger Piana di Riardo Synthem. Minor and trace element contents of samples A4, A5, A6 and A9 are closer to proximal products of Sabatini than of the Roccamonfina Synthem (Figs. 3d and 5a). Owing to their Sr–Nd isotopic signature (Fig. 6a), they can be definitely attributed to Sabatini district. For the sake of completeness, we must say that for these layers we cannot exclude *a priori* an origin from the Vulsini district, which experienced Plinian and large ignimbrite-forming eruptions in the ~590–490 ka age interval (Paleovulsini; Palladino et al., 2010; Marra et al., 2019, 2020). However, a discrimination has been possible considering the compositions of the Paleovulsini proximal to distal products, as discussed in section 5.1.2.

Samples A1, A2, A3, A7, A10, A14, A15, A17, A18a and A20 show major and trace element compositions in the range of the Sabatini and partially of the Roccamonfina products (Figs. 3 and 5). Their Cl (wt%) content mostly shows an affinity with Roccamonfina (Fig. 3d) and also isotopes are indicative of this source since all these samples show Sr and/or Nd isotopic ratios in the Roccamonfina isotopic field (Fig. 6a). Note that the isotopic compositions of A1 was not determined because the layer was visibly affected by intense clay alteration.

Based on this, hereafter, we refer to the A4, A5, A6 and A9 tephra as compositional group 1a (CG1a) and to the A1, A2, A3, A7, A10, A14, A15, A17, A18a and A20 layers as compositional group 1b (CG1b).

However, in Fig. 6, the Sabatini isotopic field has been contoured using the Sr–Nd isotopic compositions of clinopyroxene crystals only (Sottili et al., 2019), which may slightly differ from those of the bulk rock or groundmass due to open system differentiation processes. Considering the Sr and Nd isotopic values of Sabatini products younger than 490 ka (e.g., Conticelli et al., 1997, 2002; Gasperini et al., 2002; Del Bello et al., 2014) the CG1a tephra fall in the Sabatini isotopic field too. For these reasons, although they seem to show more affinity with Roccamonfina, the tephra layers of the CG1b group have been compared with products belonging to single events of the Sabatini, with the aim to definitively exclude an origin from that district.

In the following, we discuss the provenance of each tephra of these two sub-groups based on the available datasets. Hereafter, all subsequent ages are $^{40}Ar/^{39}Ar$ on sanidines, unless otherwise indicated.

5.1.2. *Compositional group 1a*

A4, A5, A6 and A9 tephra – The CG1a tephra layers show a strong geochemical affinity to the Sabatini district.

A9 – Sabatini Fall A (498.1 ± 1.6 ka)/Mercure SC3/Sulmona Sul5-1c – Based on the age and major elements glass composition, Di Rita and Sottili (2019) and Leicher et al. (2019) proposed a correlation between A9 and the Fall A (498.1 ± 1.6 ka; Marra et al., 2017) from the Tufi Terrosi con Pomici Bianche eruptive cycle (TTPB; 498.1 ± 1.6–461.0 ± 2.1 ka) of the Sabatini district (Sottili et al., 2004; Marra et al., 2014). Here we further reinforce such a correlation also based on trace element compositions and Sr–Nd isotopic ratios. The A9 major and trace element compositions well fit with that of Fall A bulk rocks and

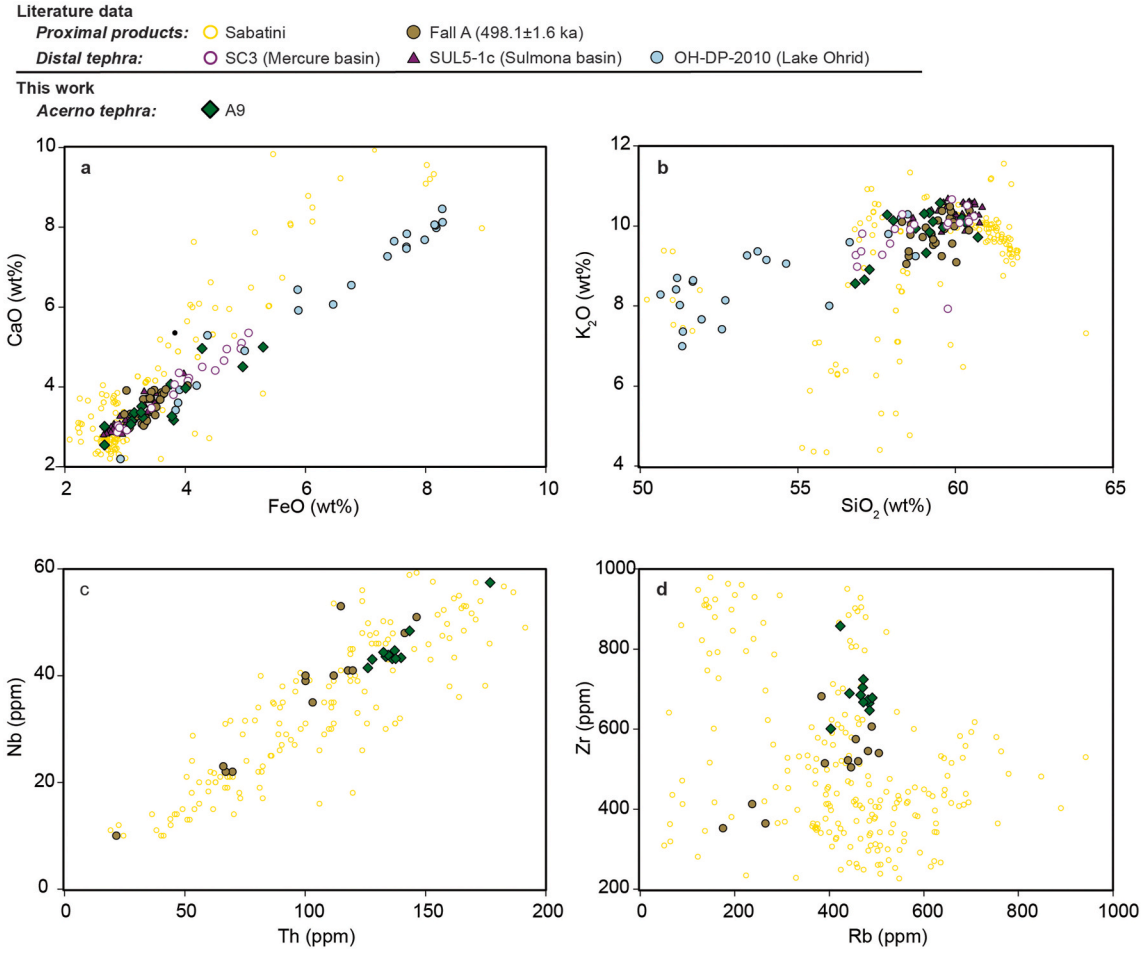

Fig. 7. a) FeO (wt%) vs CaO (wt%)- b) SiO_2 (wt%) vs K_2O (wt%)- c) Th (ppm) vs Nb (ppm) and d) Rb (ppm) vs Zr (ppm) diagrams for A9 tephra compared to Sabatini proximal products and selected tephra layers from Mercure basin, Sulmona basin and Lake Ohrid; literature data for Sabatini as in Fig. 3; for Fall A from Sottili et al. (2004), Marra et al. (2014, 2017) and Di Rita and Sottili (2019); for SC3 tephra from Giaccio et al. (2014); for Sul5-1c tephra from Giaccio et al. (2009, 2013b); for OH-DP-2010 tephra from Leicher et al. (2016, 2019).

glasses (Fig. 7).

The Sr and Nd isotopic compositions of the A9 tephra bulk rock and glass ($^{87}Sr/^{86}Sr$ = 0.71111–0.71115 and $^{143}Nd/^{144}Nd$ = 0.51210–0.51211) are very similar to those of Fall A clinopyroxenes ($^{87}Sr/^{86}Sr$ = 0.71143 and $^{143}Nd/^{144}Nd$ = 0.51210; Fig. 6b).

Hence, the stratigraphic position and the chemical and isotopic compositions point to a very reliable correlation between A9 and the Sabatini Fall A. Moreover, Fall A/A9 can be correlated with tephra layers from intermediate to distal archives of Southern Italy. They include some tephra layers found in Central Italy intramountain basins, i.e., the Sul5-1c tephra from the Sulmona basin (Giaccio et al., 2013b) and the SC3 tephra from the Mercure basin (Fig. 1b; Giaccio et al., 2014). The major element compositions of SC3 and Sul5-1c tephra well fit with that of Fall A and A9. In addition, the Sr and Nd isotopic signature of SC3 ($^{87}Sr/^{86}Sr$ = 0.71111, $^{143}Nd/^{144}Nd$ = 0.51211) is identical to that of A9 tephra ($^{87}Sr/^{86}Sr$ = 0.71111–0.71115, $^{143}Nd/^{144}Nd$ = 0.51210–0.51211) and both are close to that of Fall A ($^{87}Sr/^{86}Sr$ = 0.71143, $^{143}Nd/^{144}Nd$ = 0.51210; Fig. 6b). Another possible correlative is the OH-DP-2010 tephra from Lake Ohrid (Fig. 1b; Leicher et al., 2019), nevertheless, the latter shows a wider compositional variability (Fig. 7) compared to Fall A, A9, SC3 and Sul5-1c. Based on this, the correlation between Fall A/A9/SC3/Sul5-1c and OH-DP-2010 (Fig. 1b) can be questioned. In the light of the convincing correlation between A9 and Fall A, the dating of the latter was used as input age for the age-depth model (Supplementary Material S2).

A4, A5, A6 – Sabatini Fall C–B (490.0 ± 14.0 ka–461.0 ± 2.1 ka) – Considering the stratigraphic position of the other tephra from CG1a occurring above the A9/Fall A tephra, these can be tentatively attributed to younger products of the TTPB eruptive cycle of the Sabatini district. Therefore, A4, A5 and A6 layers are compared to the Sabatini Fall B (490.0 ± 14.0 ka) and Fall C (461.0 ± 2.1 ka; Marra et al., 2014, Fig. 1a–d in Supplementary Material S5) of the TTPB. In particular, the stratigraphic position of A6 tephra makes it the best candidate as a distal equivalent of the Sabatini Fall B. The major element composition of A6 layer is quite similar to the Fall B composition, whereas the trace element compositions of the two tephra show similarities, although do not perfectly match (Fig. 1a–d in Supplementary Material S5). Anyway, the available trace element compositions for proximal Fall B deposits are mostly based on bulk rock analyses, whereas those of Acerno data were obtained on single glass shards. This can explain the partial differences. The Fall B Sr and Nd isotopic ratios ($^{87}Sr/^{86}Sr$ = 0.71110, $^{143}Nd/^{144}Nd$ = 0.51210) are indistinguishable from those of the A6 tephra ($^{87}Sr/^{86}Sr$ = 0.71110, $^{143}Nd/^{144}Nd$ = 0.51210; Fig. 6b). Hence, a correlation between the Acerno A6 tephra and the Sabatini Fall B is considered reliable and the dating of the latter was used as input age for the age-depth model (Supplementary Material S2).

The major and trace element compositions of A4 and A5 tephra show huge differences with those of the Fall C (Fig. 1a–d in Supplementary Material S5). Also, the isotopic compositions of both A4 and A5 bulk rocks are different from that of the Fall C clinopyroxenes (Fig. 6b). Therefore, the chemical and isotopic differences do not suggest a common origin of these tephra layers with the Sabatini Fall C.

To test a possible origin from the Vulsini district, the major element contents of this set of samples has also been compared to proximal and distal coeval Vulsini products. The major element contents of A4, A5 and A6 layers do not match those of the Paleovulsini products emplaced between ~590 and 490 ka (e.g., Basal Pumices, Nenfri, Civitella d'Agliano; Nappi et al., 1987, 1995, Fig. 1a–b in Supplementary Material S5). Moreover, the trace element compositions of both Vulsini proximal products of different age and of the Lake Ohrid distal OH-DP-1998 tephra attributed to Paleovuslini by Leicher et al. (2019) differ from that of these CG1a layers (Fig. 1c–d in Supplementary Material S5), thus strongly suggesting a more probable origin from the Sabatini district.

5.1.3. Compositional group 1b

A1, A2, A3, A7, A10, A14, A15, A17, A18a and A20 tephra – At variance with the CG1a tephra, which show a strong geochemical affinity to the Sabatini district, the CG1b tephra layers show a geochemical signature better pertaining to Roccamonfina also based on their Cl (wt %) content and on the comparison with other distal tephra. The CG1b tephra layers have been compared with both Sabatini and Roccamonfina proximal to distal products, in order to undoubtedly constrain their provenance.

For the Acerno A1 and A3 tephra, no candidates have been found as possible proximal and distal counterparts.

A2 – Mercure CES1 – As illustrated in Fig. 8, the A2 tephra major element composition well fits that of CES1 tephra layer from Mercure basin (Fig. 1b; Giaccio et al., 2014).

The Sr isotopic ratio of CES1 tephra (0.70921) matches that of A2 bulk rock and glass (0.70910–0.70926; Fig. 6c). Hence, the two layers can be equivalent. The CES1 tephra has been ascribed to Roccamonfina (Giaccio et al., 2014) and the whole geochemical signature of A2 layer suggests the same source. For A2/CES1, no proximal counterpart can be evidenced to date.

Leicher et al. (2019) correlated CES1/A2 with the OH-DP-1955 tephra layer from Lake Ohrid (Fig. 1b) based on major element compositions and chronological constraints. However, although similar in composition, the latter shows some chemical differences compared to that of A2/CES1 (Fig. 8). In particular, the Cl (wt%) content of A2 and CES1 better relies with the Roccamonfina products, whereas that of OH-DP-1955 shows an affinity with the Sabatini activity (Fig. 8d).

A7– Mercure SC5 (493.5 ± 10.9 ka)/Lake Ohrid OH-DP-1966 (494.0 ± 4.4 ka) – A7, laying immediately on the top of A8, which was correlated by Petrosino et al. (2014b) to Colli Albani products dated to 500.0 ± 3.0 ka (Marra et al., 2011; recalculated at 499.2 ± 1.6 ka; Supplementary Material S2), can be correlated with SC5 from Mercure basin, dated to 493.5 ± 10.9 ka (Giaccio et al., 2014; recalculated at 491.9 ± 10.9 ka) and with OH-DP-1966 from Lake Ohrid (Fig. 1b; 494.0 ± 4.4 ka; Leicher et al., 2021). SC5 shows a bimodal composition of glasses that are phonotephritic and trachy-phonolitic (Giaccio et al., 2014) and only the latter composition partially matches the A7 glass composition. Tephra OH-DP-1966, whose glass composition well fits the SC5 trachy-phonolitic composition, also resembles the A7 composition (Fig. 8a–d). Also, the A7 trace element composition is similar to that of OH-DP-1966 (Fig. 8e–f). The $^{87}Sr/^{86}Sr$ ratio of SC5 tephra (0.70952) from Mercure basin is in the range of those of the Acerno A7 bulk rock and glass (0.70951–0.70955; Fig. 6c). Moreover, Vakhrameeva et al. (2021) proposed a possible correlation between A7/SC5/OH-DP-1966 and the cryptotephra 964B–3H-2-127.5 from the ODP site 964 (Fig. 1b). However, the reliability of this correlation is not tenable, as only a single shard of the cryptotephra was analyzed. Moreover, this cryptotephra shows some chemical differences with respect to the other tephra layers (Fig. 8). Based on these chemical differences, the correlation among A7, SC5 and OH-DP-1966 is considered consistent and that of these layers with 964B–3H-2-127.5 is considered poorly reliable. The modelled age of the correlative OH-DP-1966 was thus used as input age for the Bayesian age-depth model (Supplementary Material S2).

A10 – Mercure SC1/ZAR1 – Roccamonfina unknown – The emplacement of A10 is constrained by the age of the underlying A9/Fall A (498.1 ± 1.6 ka) and that of the overlying A11 (514.2 ± 5.6 ka; Petrosino et al., 2014b). In order to evaluate an origin from the Sabatini district, the A10 tephra composition has been compared to those of the almost coeval products from the eruptive cycles of the Grottarossa Pyroclastic Sequence (GRPS; 510.2 ± 4.1 ka) and the Tufo Giallo di Prima Porta (TGPP; 515.7 ± 1.3 ka; Marra et al., 2017). However, the GRPS and TGPP differ from A10 in their geochemical composition (Fig. 1e–f in Supplementary Material S5). Also, the Sr–Nd isotopic compositions of these products are very different from that of A10 (Fig. 6c). This in turn suggests the Roccamonfina volcano as the most plausible source for the A10 layer. Petrosino et al. (2014b) also suggested a correlation between the A10 layer and the ZAR1 layer (514.0 ± 16.0 ka; Petrosino et al., 2014a) corresponding to the SC1 tephra (516.5 ± 3.6 ka; Giaccio et al.,

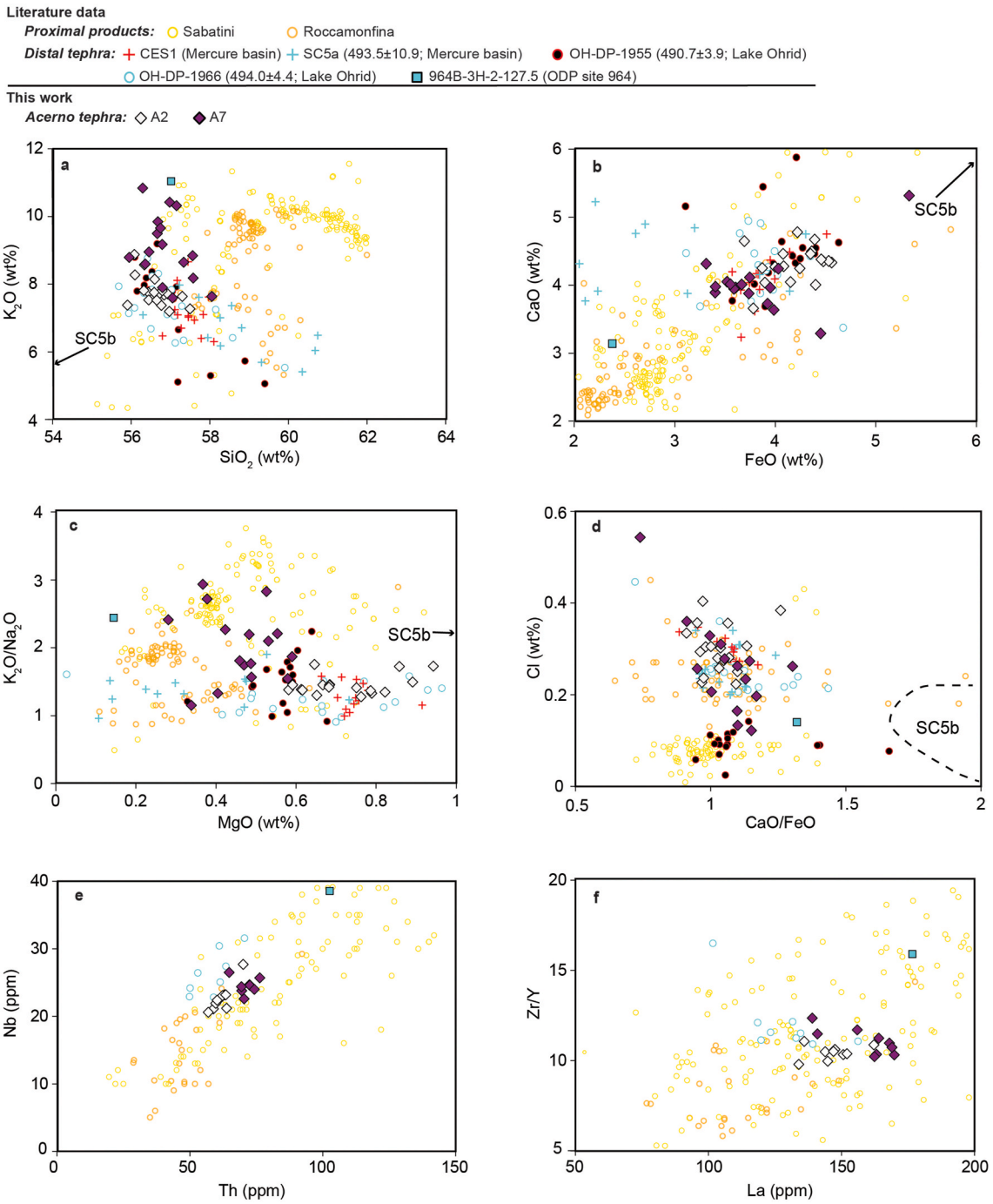

Fig. 8. a) SiO_2 (wt%) vs K_2O (wt%)- b) FeO (wt%) vs CaO (wt%)- c) MgO (wt%) vs K_2O/Na_2O- d) CaO/FeO vs Cl (wt%)- e) Th (ppm) vs Nb (ppm) and f) La (ppm) vs Zr/Y diagrams for A2 and A7 tephra layers compared to the Sabatini and Roccamonfina proximal products and tephra layers from Mercure basin, Lake Ohrid and Ionian basin; literature data for the Sabatini and Roccamonfina as in Fig. 3; for CES1 and SC5 tephra layers from Giaccio et al. (2014); for OH-DP-1955 and OH-DP-1966 tephra layers from Leicher et al. (2016, 2019); for 964B–3H-2-127.5 tephra layer from Vakhrameeva et al. (2021).

2014) of the Mercure basin (Fig. 1b). The Sr and Nd isotopic compositions of A10 bulk rock, glass and minerals are very close to that of SC1 layers (Fig. 6c); hence, A10 can be the equivalent of SC1/ZAR1.

A14, A15 – Mercure SM3, SM4 – Roccamonfina unknown – Glass compositions of A14 and A15 tephra were compared to the products from the Sabatini district emplaced between the age of A11 (514.2 ± 5.6 ka) and that of A16 (561.7 ± 11.8 ka; Petrosino et al., 2014b): these are the Lower Tufo Giallo della Via Tiberina (LTGVT; 549.0 ± 16.0 ka; Marra et al., 2014), the Upper Tufo Giallo della Via Tiberina (UTGVT; 545.5 ± 3.0 ka; Marra et al., 2014, 2017) and the TGPP (515.7 ± 1.3 ka). The chemical and isotopic compositions of both A14 and A15 are different from that of the TGPP (Fig. 6c; Fig. 1g–h in Supplementary Material S5).

The major elements composition of A14 matches that of the UTGVT, whereas that of A15 does not match that of the UTGVT and only partially matches that of the LTGVT (Fig. 1g–h in Supplementary Material S5).

The major elements composition of A14 layer also fits quite well that of the SM4 tephra from the Mercure basin (Fig. 1g–h in Supplementary Material S5), as well as the Sr-isotopic composition of feldspar crystals of A14 layer is very close to that of SM4 tephra (Fig. 6c). Also based on

their stratigraphic position, these layers can be equivalent, as already suggested by Giaccio et al. (2014) (Fig. 1b). On the other hand, the Sr-isotopic compositions of both A14 and A15 are distinctively different from that of the UTGVT (Fig. 6c). Based on this, the correlation proposed by Petrosino et al. (2014b) between A14/A15 and UTGVT (Fig. 2) has to be disproved.

The LTGVT shows major elements composition and Sr and Nd isotopic ratios slightly different from that of the A15 tephra (Fig. 6c; Fig. 1g–h in Supplementary Material S5). The SM3 tephra from the Mercure basin (Giaccio et al., 2014) shows chemical and Sr-isotopic compositions quite similar to those of A15 tephra (Fig. 6c; Fig. 1g–h in Supplementary Material S5). For these reasons and for their stratigraphic positions, these two layers can probably be equivalents or be originated from almost coeval events from the same source. The SM4 and SM3 tephra were attributed to the Roccamonfina activity and, since none of the Sabatini products erupted in the considered time span is fully compatible with the A14 and A15 tephra, these layers can be likely originated from Roccamonfina, also in agreement with their Cl (wt%) content (Fig. 3d) and isotopic ratios (Fig. 6a–c).

A17, A18a, A20 – Roccamonfina unknown, Mercure SL2 (>561 ka) – The A17, A18a and A20 tephra from CG1b are chronologically constrained between 561.7 ± 11.8, age of A16, and 557.0 ± 9.7 ka, age of A20. They can be thus compared to the First Ash Fall Deposits of the Sabatini district that correspond to a series of eruptive events which occurred at ~590–540 ka (FAD; Marra et al., 2014). However, the FAD products have chemical compositions quite different from those of these layers (Fig. 1i-l in Supplementary Material S5). Moreover, the Sr-isotopic composition of the FAD clinopyroxenes (0.71143 and 0.71150; Sottili et al., 2019) is sensibly higher than that measured on the A17 (0.70971–0.70978), A18a (0.70971–0.70977) and A20 (0.70996) tephra layers (Fig. 6c). Moreover, notwithstanding the A17, A18a and A20 emplacement can be close to that of the LTGVT (549.0 ± 16.0 ka), their isotopic compositions are completely different.

The A17, A18a and A20 layers can be compared also to the Mercure basin tephra older than ~520 ka attributed to Roccamonfina (Fig. 1b; Giaccio et al., 2014). However, none of the described Mercure tephra can be identified as a counterpart of A17. The major element composition of tephra A18a shows a partial fit with the SM1 tephra from Mercure basin (Fig. 1b; Fig. 1i-l in Supplementary Material S5), but the latter shows a wider compositional variation. Similarly, the Sr–Nd isotopic compositions of the two tephra are slightly different (Fig. 6c). For these reasons, although having a similar stratigraphic position, a correlation between the two tephra cannot be established.

The Mercure SL2 major element and isotopic compositions well match those of A20 (Fig. 1b; Fig. 6c; Fig. 1i-l in Supplementary Material S5). This layer has been attributed to a pre-Rio Rava (~438 ka, Rouchon et al., 2008) event of Roccamonfina (Giaccio et al., 2014). The Sr isotopic composition of the two tephra is quite similar (Fig. 6c). The two tephra can be considered equivalent also according to their stratigraphic position.

Even if no proximal counterparts have been found for A17, A18a and A20 tephra, their Cl (wt%) content and their isotopic ratios indicate a provenance from Roccamonfina rather than Sabatini district (Fig. 1l in Supplementary Material S5; Fig. 6), as for the other tephra of CG1b. As a matter of fact, to corroborate the occurrence of explosive activity of this age at the Roccamonfina volcano, both Valente et al. (2019) and Boncio et al. (2022) found a tephra layer at the footslopes of the Matese mountain front, attributed to the early stages of activity of the volcano, dated at 564.9 ± 2.4 ka and 564.5 ± 2.1 ka, respectively, which corresponds within the error to the age found here for tephra A20. Furthermore, in Bojano basin, a tectonic depression relatively close to the Roccamonfina volcano, a tephra layer dated at 582.0 ± 2.0 ka was also tentatively attributed to an early Roccamonfina activity (Galli et al., 2017). Unfortunately, none of these ancient Roccamonfina tephra yielded fresh glass suitable for geochemical analyses, leaving indefinite the possible correlation with A20.

5.1.4. CG2 tephra

A8, A13 and A19 tephra – The foiditic and phono-tephritic samples of the Acerno succession are characterized by notably higher CaO (wt %), FeO (wt%), MgO (wt%), Ni (ppm) and V (ppm) contents and lower SiO_2 (wt%) contents with respect to those of the other CGs (Fig. 3). The major element contents of A8 and A19 layers distinctly indicate a provenance from the Colli Albani district (Fig. 3), whose activity was characterized by at least four explosive events in the 560–500 ka time span (Marra et al., 2009). The trace element contents of these samples support the major element signature: the higher compatible trace element contents (e.g., V; Fig. 5c) and La/Yb ratios allow distinguishing these samples from the other CGs. Although the compositional fields do not completely overlap, the trace element trend of these samples shows a clear affinity with that of the Colli Albani products (Fig. 5). Besides, CG2 samples fall in the area where the Colli Albani and Sabatini Sr–Nd isotopic fields overlap (Fig. 6a). However, their major and trace elements contents undoubtedly indicate a compositional affinity with the Colli Albani products.

A8 – Colli Albani Ash Fall succession (AF-d; 500.0 ± 3.0 ka)/ Mercure SC4 – Petrosino et al. (2014b) hypothesized a correlation of the A8 layer with the products of the last activity of the eruptive cycle of Colli Albani known as Ash Fall succession. These deposits, also known as TBA-PRSF (Fig. 2), are sandwiched between the Tufo di Bagni Albule (TBA; 527.0 ± 2.0 ka; Marra et al., 2009) and the Pozzolane Rosse Scoria Fall (PRSF; 456.0 ± 3.0 ka; Karner et al., 2001, re-calculated in Marra et al., 2009), and comprise six eruptive units (AF-a to AF-f) dated between ~517 and 500 ka correlated to the Sabatini and Colli Albani activities (Marra et al., 2009). We strengthen such a correlation, based on glass major elements, Sr-isotopic composition and stratigraphic constraints: the major element glass compositions of the Ash Fall succession from proximal outcrops (AF-d; Marra et al., 2009; Giaccio et al., 2013a) fit in part with that of the A8 bimodal tephra (Fig. 9).

The isotopic composition of A8 glass is very close to that of bulk rock analyzed in the Ash Fall succession at intermediate sites (Sulmona basin) by Giaccio et al. (2013a) (Fig. 6d). Moreover, since A9 corresponds to the Sabatini Fall A (498.1 ± 1.6 ka), which, in proximal areas, is embedded between the AF-a (517.0 ± 1.0 ka) and AF-c (<500.0 ± 3.0 ka; Sottili et al., 2004; Marra et al., 2009), it is very probable that A8 has been originated from one of the events that emplaced the uppermost part of the Ash Fall succession. Moreover, the A8 major element composition, although not perfectly matching, is similar to that of the SC4 tephra from the Mercure basin (Fig. 1b; Fig. 9), that has been ascribed by Giaccio et al. (2014) to the AF-d products (500.0 ± 3.0 ka; Marra et al., 2009, 2011). The mismatch in the major element contents between SC4 and A8 tephra can be explained by a possible analytical bias. The major element variations of the two tephra also show the same trend. Besides, the Sr–Nd isotopic composition of SC4 ($^{87}Sr/^{86}Sr$ = 0.71065 and $^{143}Nd/^{8144}Nd$ = 0.51213) well fits with that of A8 layer ($^{87}Sr/^{86}Sr$ = 0.71059 and $^{143}Nd/^{8144}Nd$ = 0.51211; Fig. 6d), hence the two tephra can be considered equivalents.

A13 – Colli Albani (AF-a?) – The A13 layer was attributed by Petrosino et al. (2014b) to a generic Latium source. The silica undersaturated composition and the high CaO content (12–10 wt%) would make it possible to hypothesize a Colli Albani source. Nevertheless, all the Colli Albani products erupted between TPT/A19 and AF-d/A8 (e.g., Tufo del Palatino, Tufo di Bagni Albule; Marra et al., 2009) known to date differ from the A13 layer composition (Fig. 1 in Supplementary Material S6). From a stratigraphic point of view, a correlation with the older Ash Fall deposit AF-a (517.0 ± 1.0 ka) can be proposed. However, a definite attribution is hampered as this part of the Colli Albani proximal succession is currently incompletely characterized and the lack of analyzable glasses in the AF-a unit (Marra et al., 2009) precludes a geochemical correlation.

A19 – Colli Albani Tufo Pisolitico di Trigoria (TPT; 561.2 ± 2.0 ka)/Mercure SL3 – The A19 layer from CG2, chronologically constrained between 561.7 ± 11.8, age of A16, and 557.0 ± 9.7 ka, age of

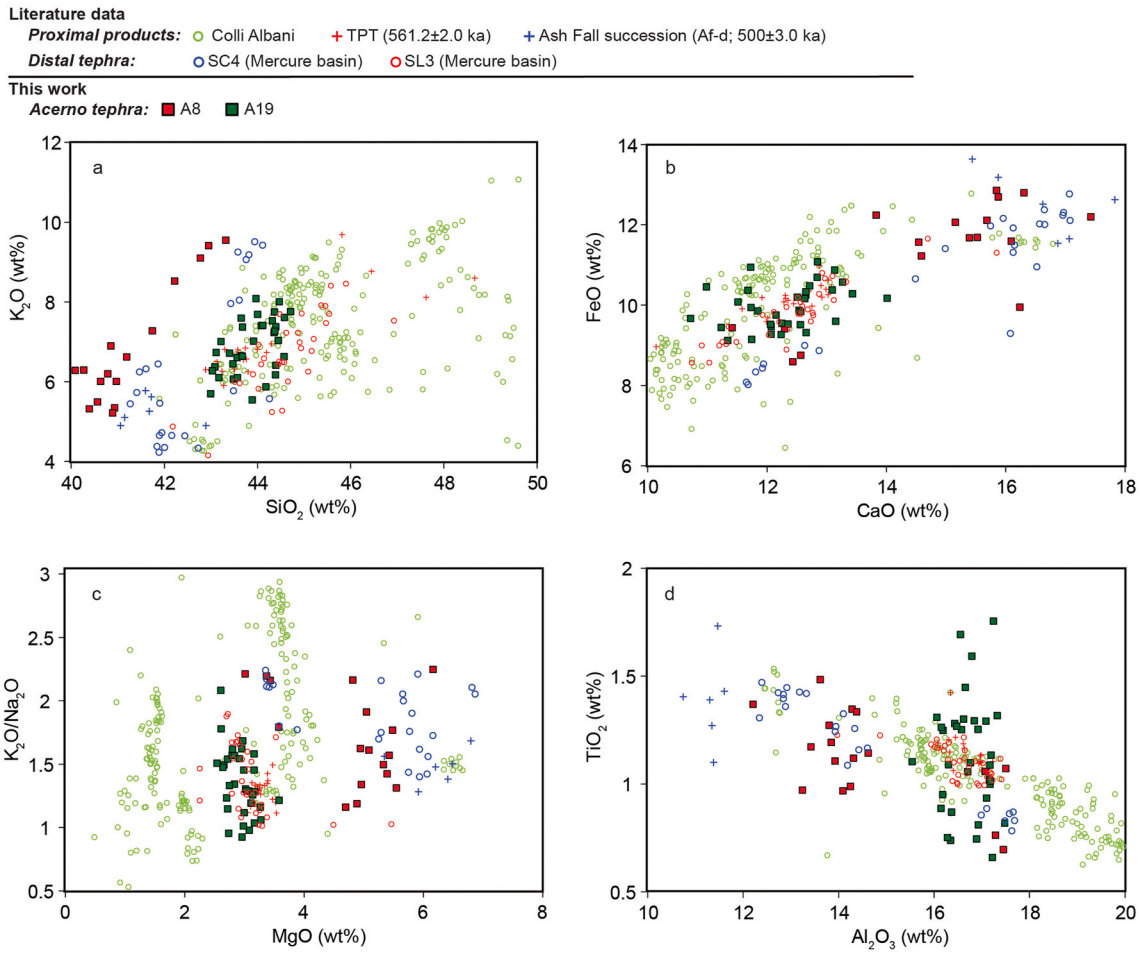

Fig. 9. a) SiO_2 (wt%) vs K_2O (wt%)- b) FeO (wt%) vs CaO (wt%)- c) MgO (wt%) vs K_2O/Na_2O and d) Al_2O_3 (wt%) vs TiO_2 (wt%) diagrams for A8 and A19 tephra compared to Colli Albani proximal products and tephra layers from Mercure basin; literature data for Colli Albani as in Fig. 3; for Ash-Fall successions and TPT from Palladino et al. (2001), Gaeta et al. (2006), Marra et al. (2009) and Giaccio et al. (2013a); for SC4 and SL3 tephra from Giaccio et al. (2014).

A20, was attributed by Petrosino et al. (2014b) to the Tufo Pisolitico di Trigoria (TTC; Palladino et al., 2001; TPT; Giaccio et al., 2013b; 561.2 ± 2.0 ka recalculated at 566.7 ± 2.0 ka; Supplementary Material S2) from Colli Albani, based on the perfectly matching major element chemical compositions (Fig. 9). This correlation is here further strengthened by its bulk rock Sr–Nd isotope compositions ($^{87}Sr/^{86}Sr$ = 0.71121 and $^{143}Nd/^{8144}Nd$ = 0.51212), which is fully consistent with that of TPT ($^{87}Sr/^{86}Sr$ = 71104–0.71131 and $^{143}Nd/^{144}Nd$ = 0.51212; Fig. 6d; Gaeta et al., 2006). Here, we further constrain the correlation between the A19 and the Mercure SL3 layer (Giaccio et al., 2014), based on chemical and isotopic evidence (Figs. 6d and 9).

5.1.5. *CG3 tephra*

A11, A12, A16 and A18b tephra – The A11, A12 and A16 trachytic samples and the A18b phonolitic sample of CG3 show higher SiO_2 (wt%) and lower CaO (wt%) contents and CaO/FeO ratios with respect to those of the other CGs (Fig. 3). The major and trace element contents of these samples resemble those of products from the Pontian islands, Campi Flegrei, Somma-Vesuvius and Ischia island (Figs. 3 and 5), particularly exhibiting affinity with Ischia products erupted in the last 150 ka (Fig. 10).

Although in near-vent areas there is little or no testimony for the Middle Pleistocene explosive activity of the Neapolitan Volcanic Area, a growing set of evidence from distal settings testifies to the occurrence of pyroclastic products similar in composition to those erupted from Campi Flegrei, Somma-Vesuvius and Ischia island in the Late Pleistocene-Holocene period (Giaccio et al., 2012; Insinga et al., 2014; Petrosino et al., 2015, 2019; Leicher et al., 2021; Monaco et al., 2022b). These could belong to a possible older phase of activity in the Neapolitan Volcanic Area before the onset of the volcanic activity of the present-day Campi Flegrei, Somma-Vesuvius and Ischia island.

The Cl (wt%) content of these tephra indicates an origin from either the Pontian islands or the Neapolitan Volcanic Area as well, and an affinity with the Ischia island compositions (Figs. 3d and 10d). The partial match, however, can be due to a lack of data for the proximal products, in particular for old products from the Neapolitan Volcanic Area. The Sr–Nd isotopic compositions of the A11, A12, A16 and A18b tephra layers also show affinity with the proximal products from the Pontian islands, Campi Flegrei, Somma-Vesuvius and Ischia island too (Fig. 6). For the A18b sample, a possible explanation for the different Sr–Nd ratios between glass and feldspars can be either an isotopic disequilibrium related to open-system processes or the contribution of xenocrysts/antecrysts with isotopic composition different from that of the host rock.

The trace elements of the tephra belonging to CG3 record compositions and variation trends comparable to the Pontian islands, Campi Flegrei, Somma-Vesuvius and Ischia island (Fig. 5). However, some differences exist in the glass composition of these tephra: A11 and A12 are rather homogeneous in terms of major and trace elements. A16 trace elements reveal a compositional bimodality: one fitting the A11 and A12 compositions (trachyte), and another resembling the A18b composition (phonolite) which is characterized by slightly higher Th, Nb, Rb, Sr and Ba contents and notable Ba and Sr negative peaks in the spider diagram, with respect to that of A11 and A12 tephra (Figs. 4 and 5). Based on their isotopic signature, A11 and A12 mostly show an affinity with the

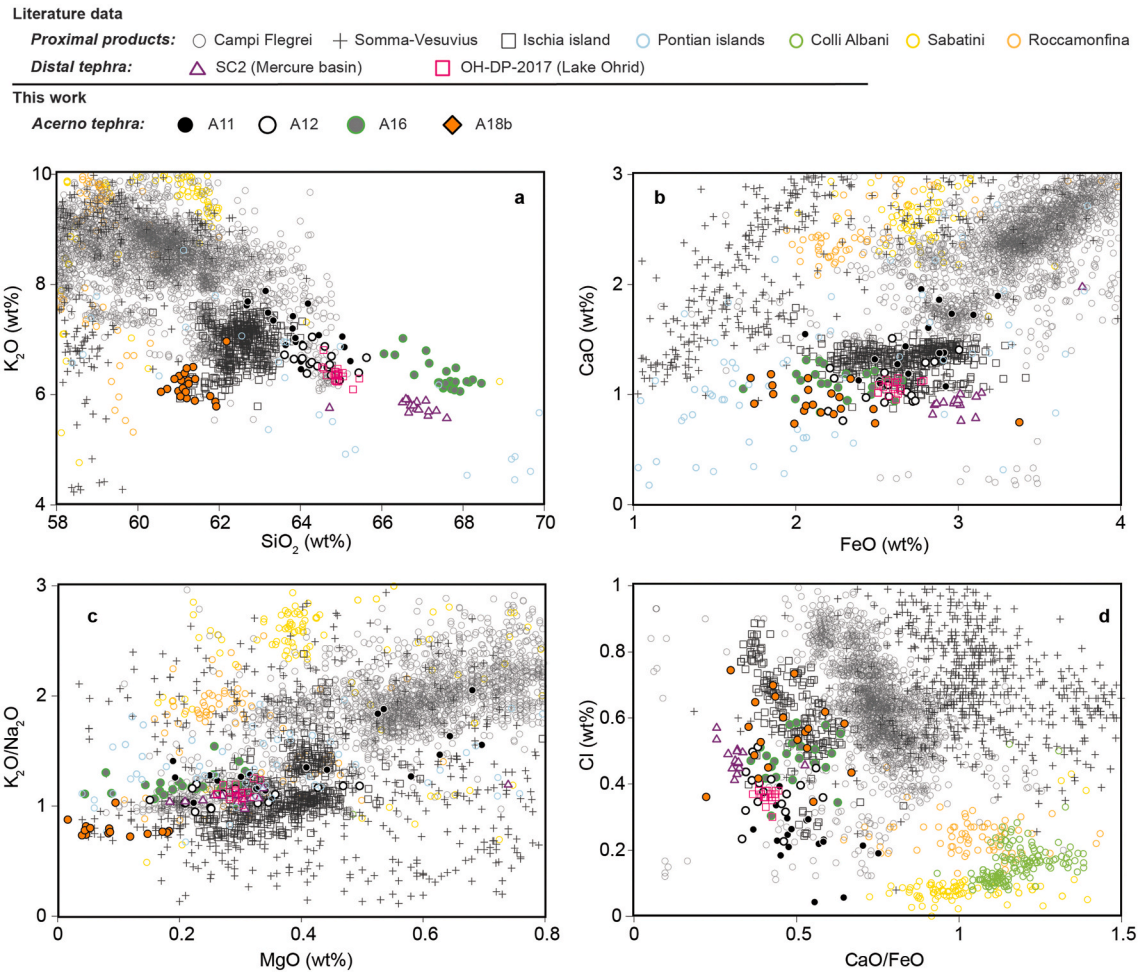

Fig. 10. a) SiO_2 (wt%) vs K_2O (wt%)- b) FeO (wt%) vs CaO (wt%) and c) MgO (wt%) vs K_2O/Na_2O and d) CaO/FeO vs Cl (wt%) diagrams for the A11, A12, A16 and A18b tephra compared to Colli Albani, Roccamonfina, Sabatini, Pontian islands, Campi Flegrei, Somma-Vesuvius and Ischia island proximal products and tephra layers from Mercure and Lake Ohrid; literature data for the Colli Albani, Roccamonfina, Sabatini, Pontian islands, Campi Flegrei, Somma-Vesuvius and Ischia island as in Fig. 3; data for the SC2 tephra from Giaccio et al. (2014); data for the OH-DP-2017 tephra from Leicher et al. (2019).

Neapolitan Volcanic Area, whereas A16 and A18b with the Pontian islands. Nevertheless, we cannot exclude that A16 has been originated by the Neapolitan Volcanic Area and therefore we could hypothesize that the older products had isotopic compositions different from the current ones. This would also imply an isotopic time-dependent variability for this source as that observed in the Colli Albani (Gaeta et al., 2006; Giaccio et al., 2013a).

A11/A12 – Ohrid OH-DP-2017 – Giaccio et al. (2014) hypothesized a correlation between A11/A12 and SC2 from Mercure basin (Fig. 1b), whose age is constrained by the underlying SC1 layer (516.5 ± 3.6 ka). However, if SC1 is the equivalent of A10, as proposed in section 5.1.3, then the correlation between A11/A12 and SC2 is not possible based on stratigraphic criteria, because SC2 is above SC1, while A11/A12 are below A10 and its Mercure equivalent SC1 (Fig. 1b). Indeed, the A11 and A12 tephra show major element compositions different from that of SC2 tephra from the Mercure basin (Fig. 10). This would imply that at least two explosive eruptions originated from the Neapolitan Volcanic Area in a short time span. On the other hand, the A11 and A12 major element compositions are more similar to that of the OH-DP-2017 layer from the Lake Ohrid (Fig. 1b: Fig. 10). Hence, also based on their stratigraphic positions, these layers can be possibly considered equivalent, as already hypothesized by Leicher et al. (2019).

A18b – Ventotene – Petrosino et al. (2019) noticed that major element glass composition of A18b is comparable with those of Ventotene proximal products (e.g., Parata Grande eruption; Bellucci et al., 1999), belonging to the Pontian islands. Sr–Nd isotopic ratios strongly suggest a potential attribution of this sample to the Ventotene activity as well (Fig. 6).

5.2. *Modelled age for the Acerno tephra*

The above discussed correlations of the Acerno tephra allow adding further $^{40}Ar/^{39}Ar$ dating to those already available performed on the A3, A11, A16 and A20 tephra (Petrosino et al., 2014b). Specifically, the following five convincing tephra correlations were used for integrating the input dataset used for the Bayesian age-depth model: A6/Sabatini Fall B (490.0 ± 14.0 ka), A7/Mercure SC3 (491.9 ± 10.9), A8/Colli Albani AF-d (498.0 ± 3.0), A9/Sabatini Fall A (499.2 ± 1.6 ka) and A19/Colli Albani TPT (561.2 ± 2.0 ka) (Fig. 11).

In addition to the direct and indirect $^{40}Ar/^{39}Ar$ chronology, the attribution of the Acerno record to the 570-470 ka interval is also confirmed by the expression of the orbital and sub-orbital paleoenvironmental-climatic variability of the Acerno pollen record, which shows significant resemblance with that shown by the Lake Ohrid pollen during the late MIS 15-late MIS 12 period (Fig. 11). Therefore, by assuming that the observed changes in pollen assemblages are an expression of the near-synchronous, central Mediterranean regional-scale climate variability, we aligned the depth-series of the Acerno arboreal pollen (minus *Pinus*, AP-*Pinus*) with the homolog time-series from Lake Ohrid, along six tie-points (blue lines in Fig. 11). The main, first-order tie-points

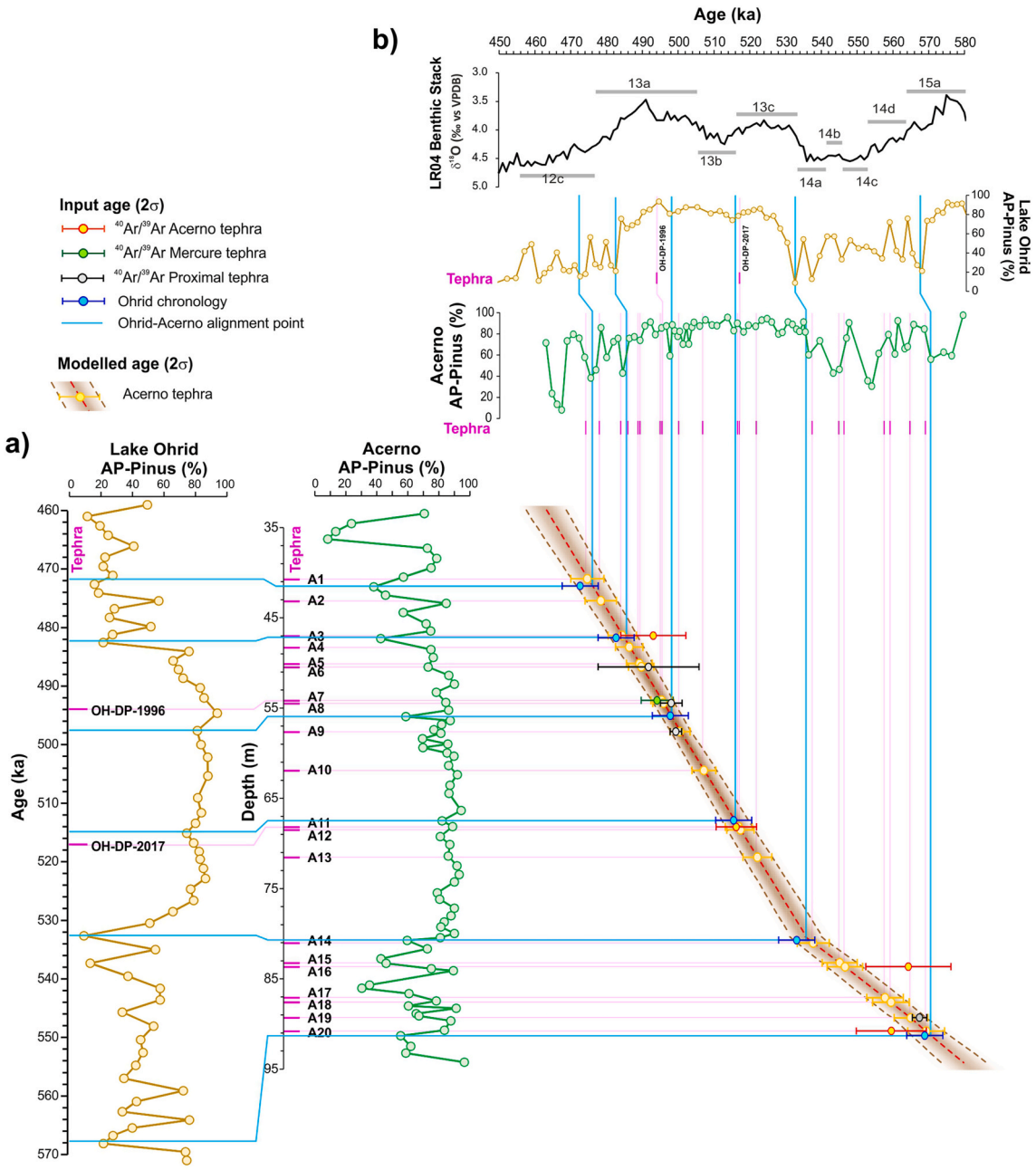

Fig. 11. Age-depth model of the Acerno tephra; a) Alignment of the Ohrid AP-*Pinus* pollen curve (Kousis et al., 2018; Wagner et al., 2019; Donders et al., 2021) with the Acerno AP-*Pinus* pollen curve (Russo Ermolli, 2000; Munno et al., 2001) and Bayesian age-depth model, including direct (Acerno tephra) and indirect (correlated tephra) $^{40}Ar/^{39}Ar$ ages and the Ohrid ages deriving from the alignment of Ohrid and Acerno pollen records; b) Resulting time-series of the Acerno pollen and tephra records compared with Ohrid pollen record (Kousis et al., 2018; Wagner et al., 2019; Donders et al., 2021) and the LR04 benthic stack $\delta^{18}O$ record (Lisiecki and Raymo, 2005).

correspond with lower and upper boundaries of the more stable and longer period showing clear interglacial features, occurring in Acerno between ~78 m and ~46 m and between ~432 ka and ~482 ka, roughly matching the MIS 13 interglacial (Fig. 11). Two other tie-points where identified within the MIS 13 interglacial and correspond to two stadial oscillations clearly identifiable in both records (~68 m and ~56 m in Acerno, ~515 ka and ~498 ka in Ohrid; Fig. 11). Finally, two further tie-points correspond with two marked stadials in MIS 14 and MIS 12 (~88 and ~43 m in Acerno, ~568 ka and 473 ~ka in Ohrid) and we transferred their ages into the Acerno record.

This alignment allowed transferring six further ages from Ohrid chronology (Wagner et al., 2019) to the input dataset used for the Bayesian age-depth model. The resulting age-depth model, including the additional five $^{40}Ar/^{39}Ar$ dating from correlated tephra and the six tie-points from Ohrid chronology, allows us to reliably assign to each individual Acerno tephra modelled ages, with their own statistically significant uncertainty, expressed as 2σ, as summarized in Fig. 12 (for details see Supplementary Material S2).

The modelled ages range from 474.3 ± 4.6 ka, age of A1, to 568.8 ± 5.1 ka, age of A20. In particular, A1 and A2 are found in glacial sediments associated with the MIS 12, twelve tephra layers, from A3 to A14, are associated with the MIS 13, five layers, from A15 to A18b, are located in the MIS 14, and A19 and A20 layers seem associated with the late MIS 15, notwithstanding the latter is not well represented by the Acerno pollen record.

The modelled ages of tephra that have not been directly dated

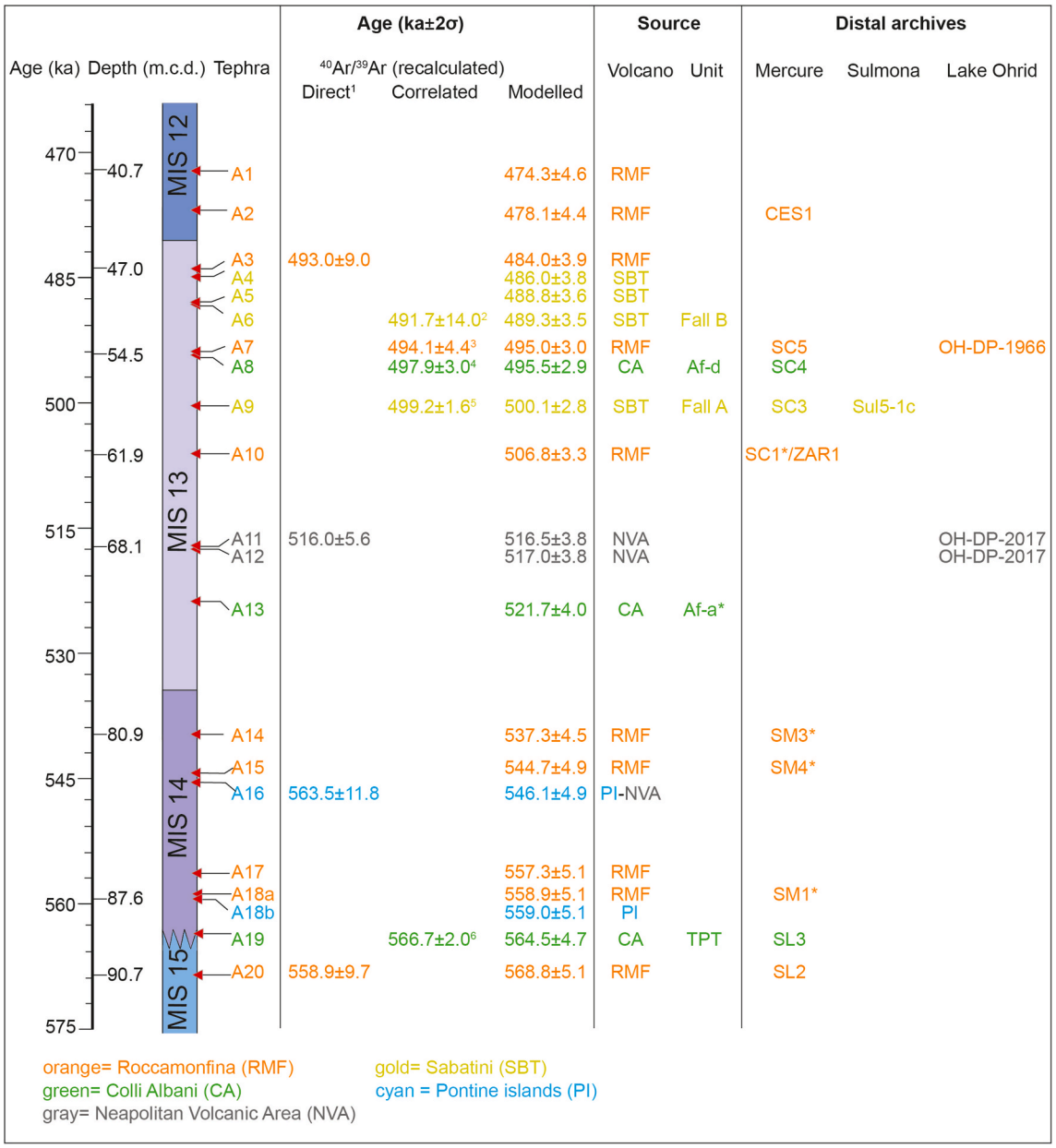

Fig. 12. Tephrostratigraphy of the Acerno succession. The position of tephra layers (arrows) along with depth and the MIS (boundaries from Lisiecki and Raymo, 2005). Attributions to the volcanic source and to a specific eruption (with the recalculated age) are given for the tephra layers together with their direct $^{40}Ar/^{39}Ar$ age and modelled age. A summary of proposed correlations of the Acerno tephra with distal archives across central-southern Italy and the Mediterranean is reported. The different colors used for labelling the tephra layers correspond to their different volcanic origins. *Possible correlation; [1]Petrosino et al. (2014b), [2]Marra et al. (2014), [3]Giaccio et al. (2014), [4]Marra et al. (2009), [5]Marra et al. (2017), [6]Karner et al. (2001) recalculated in Marra et al. (2009). (For interpretation of the references to color in this figure legend, the reader is referred to the Web version of this article.)

through $^{40}Ar/^{39}Ar$ or by age-transfer of correlated, dated equivalents are also useful to give constraints on some distal inter-archive correlations. For instance, the OH-DP-2010 tephra from Lake Ohrid, tentatively correlated to FallA/A9 (Leicher et al., 2019), shows an older modelled age (514.2 ± 4.4 ka; Leicher et al., 2021) compared to those of the Fall A (498.1 ± 1.6 ka) and A9 (500.1 ± 2.8 ka), besides the different compositional variability (Fig. 7). This provides further evidence against the previously proposed correlation (Fig. 1b).

Similarly, the OH-DP-1955 tephra from Lake Ohrid shows an older modelled age (Fig. 1b; 490.7 ± 3.9 ka; Leicher et al., 2021) compared to that of A2 (478.1 ± 4.4 ka), which would also imply an emplacement in very different climatic conditions (MIS 13 vs MIS 12). Hence, although having quite similar glass composition, the two layers likely represent the distal counterpart of two different events.

The modelled age of A10 (506.8 ± 3.3 ka) is statistically indistinguishable from the low precision age of ZAR1 layer (514.0 ± 16.0 ka; Petrosino et al., 2014a), while, within 2σ uncertainty, it is substantially younger than the age of SC1 tephra (516.5 ± 3.6 ka; Giaccio et al., 2014) of the Mercure basin. Therefore, while the modelled age of A10 could confirm a correlation between A10 and the Mercure ZAR1, it could not support the correlation with Mercure SC1 (Fig. 1b).

Finally, the A13 modelled age (521.7 ± 4.0 ka) also fits within error with the age of the AF-a (517.0 ± 1.0 ka). Therefore, although a correlation solely based on geochemical signature is not feasible, the modelled ages provide additional support for a correlation between the two tephra layers.

5.3. The Acerno basin in the Mediterranean tephrostratigraphic framework and implications for the Middle Pleistocene Italian volcanic activity

Together with stratigraphic and age constraints, the geochemical dataset on the twenty-one tephra layers of the Acerno lacustrine succession, clustered in three different CGs, allowed some robust correlations with the Italian volcanic sources (Fig. 12), providing new insights into the explosive activity of the peri-Tyrrhenian volcanoes during the MIS 15–12.

In this context, the lack of a suitable geochemical characterization on proximal products, in particular for the ancient stage of activity of some volcanic complexes (e.g., Neapolitan Volcanic Area), makes the attribution and correlations challenging. For this reason, the characterization of distal tephra becomes essential to shedding light on the eruptive history of these volcanic complexes.

Moreover, together with chronological indication and major and trace elements characterization, the tephrostratigraphic methods would benefit from the employment of radiogenic isotopes, as clearly shown for the Acerno tephra. The Sr and Nd isotopic ratios turned out to be a very useful tool indicative of the source for all the Acerno tephra. Their use allowed providing reliable attributions and strengthening the proximal-distal tephra correlation, as well as making consistent inter-archive correlations (e.g., A8/SC4, A9/SC3, A19/SL2). Also, their use allowed the reappraisal of some previously proposed attributions (Fig. 1b; e.g., A14/A15/UTGVT; Petrosino et al., 2014b). The occurrence of certain tephra layers at Sulmona, Mercure and even Ohrid, which were not detected in the Acerno basin, as well as vice versa, could be partly attributed to the fact that only visible tephra were analyzed in all these successions. By investigating cryptotephra, the tephra framework should become more comprehensive and better comparable in these successions, notwithstanding the differences in sedimentation rate, preservation degree and, most importantly, in the dispersal direction of the pyroclastic clouds, which strongly influence distal and ultradistal tephra deposition.

Overall, the Acerno tephra layers were mainly sourced at the Latium volcanoes or at Roccamonfina, for which the Acerno record currently represents the richest distal archive for the investigated, ~100 kyr-long, time-span between ~570 ka and ~470 ka. In addition to provide new insights for the explosive history of these main volcanic sources, the Acerno tephra archive also sheds new light on either a currently geochronologically poorly constrained history of the Pontian islands or a completely unknown, ancient explosive activity in Neapolitan Volcanic area.

The CG1a includes four - out of twenty-one - tephra emplaced by the Sabatini district (Fig. 12). Even in this case, the lack of a full geochemical characterization of proximal products of the ~500–490 period, except for the A9/Fall A and, in part, for the A6/Fall B, does not allow a precise attribution to a specific event. The A9/Fall A tephra, also found in the distal successions of Mercure and Sulmona basins (Fig. 13), candidates as a good tephra marker for MIS 13 in the Italian peninsula.

The CG1b includes ten - out of twenty-one - layers likely originated from the Roccamonfina stratovolcano (Fig. 12), establishing it as the main volcanic source of the Acerno tephra.

Although the beginning of the volcanic activity at Roccamonfina is not well constrained, the oldest pyroclastic deposits sampled from a deep borehole drilled at the center of the present caldera yield an age of ~630 ka (Ballini et al., 1989), which represents the onset of the Roccamonfina Synthem (De Rita and Giordano, 1996). This period of activity is still not well-characterized with respect to the subsequent Piana di Riardo Synthem (<410 ka). In this regard, the abundance of CG1b tephra, some of which also occur in other distal successions (e.g.,

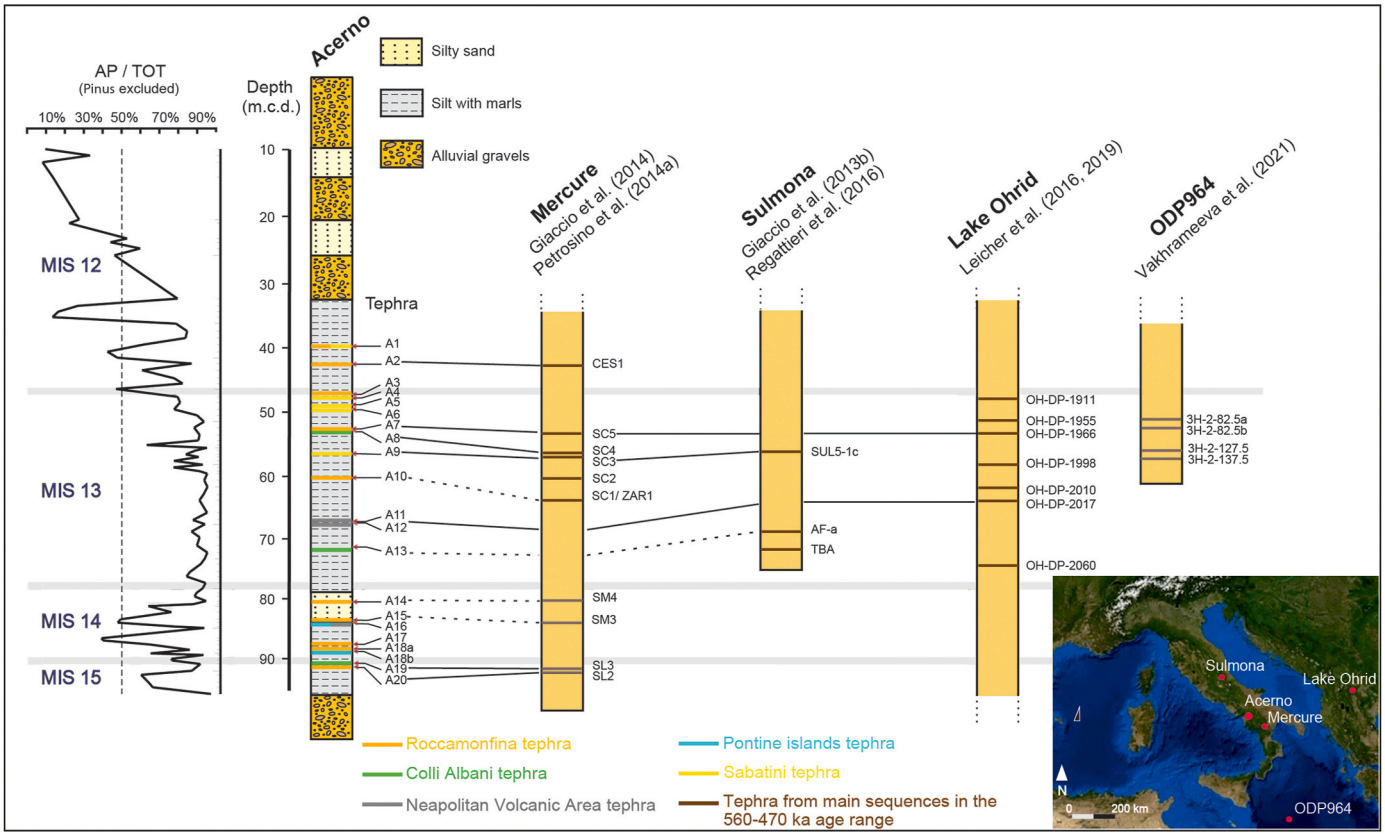

Fig. 13. Tephrostratigraphic framework of Acerno and selected distal archives with tephra in the ~570–470 ka time span. Tephra layers are shown along with Acerno's proxy data (Petrosino et al., 2014b). Solid lines indicate robust correlations and black dashed lines indicate possible correlations. Glacial/interglacial transitions are indicated by gray lines.

A2/CES1, A7/SC5/OH-DP-1966, A10/SC1/ZAR1 and A20/SL2; Fig. 13) provides evidence for a conspicuous, yet still not well-defined in proximal areas, Middle Pleistocene explosive activity at Roccamonfina volcano.

The CG2 includes three - out of the twenty-one - Acerno tephra layers, which were likely generated from the Colli Albani district. In particular, the confident correlations among A8/AF-d and A19/TPT with other layers from distal tephra archives (Mercure, Sulmona basins) testify to their wide dispersal over the Italian peninsula (Fig. 13). This feature and their distinctive geochemical composition make them important marker horizons for the ~570–500 ka period. Furthermore, enhancing the geochemical characterization of their proximal counterparts would facilitate a more accurate reconstruction of the dispersal of Colli Albani tephra resulting from explosive activity during this time span. This is underscored by the tentative attribution of the A13 tephra to the AF-a.

The CG3 includes four out of twenty-one tephra showing geochemical affinity with the Pontian islands, Campi Flegrei, Somma-Vesuvius and Ischia island products (Fig. 12). In particular, the A11/A12 tephra, likely originated from the Neapolitan Volcanic Area source was considered by Petrosino et al. (2014) as the product of a high magnitude eruption due to its considerable thickness (c. 30 cm) and coarse grain size of fragments (max 5 mm diameter). Its occurrence in the Lake Ohrid succession (OH-DP-2017; Fig. 13), situated 600 km east of the possible source, can confirm the huge size of the explosive event. Also, the Acerno A16 and the Mercure SC2 events can testify to a conspicuous activity from this not well constrained source in the same time span. In the light of these considerations, the onset of activity in the Neapolitan Volcanic Area appears to be much older than currently recognized.

6. Summary and concluding remarks

Trace element and Sr–Nd isotope data acquired in this study completed the geochemical dataset of twenty-one tephra from the Acerno lacustrine succession, previously characterized only in terms of glass major element composition and $^{40}Ar/^{39}Ar$ geochronology. Based on this full geochemical fingerprinting, the Acerno tephra layers have been distinguished into three compositionally different groups.

CG1a - Sabatini and CG1b - Roccamonfina - The sources of CG1 tephra, previously attributed to the Middle Pleistocene activity of Sabatini district or Roccamonfina volcano, have been more precisely assessed. The CG1a tephra layers (A4, A5, A6 and A9) have been confidentially ascribed to the Sabatini district, mostly based on their Sr and Nd isotopic compositions. Additionally, the trace element contents of these tephra are rather homogeneous and overlap with the compositions of the Sabatini proximal products. In particular, the A9 tephra is a distal counterpart of the Sabatini Fall A (498.1 ± 1.6 ka), whose products are dispersed in several proximal to distal localities (Mercure and Sulmona basins). The chemical and isotopic signatures of most of the CG1b samples (A1, A2, A3, A7, A10, A14, A15, A17, A18a and A20) indicate Roccamonfina as the most likely source of these tephra, among which, A2, A7, A10, A14, A15 and A20 tephra have some possible equivalents in other sedimentary archives in Southern Italy and/or in the Mediterranean area. The identification of the Roccamonfina volcano as the most probable source suggests that this volcanic district has experienced a still poorly known intense and frequent explosive activity during the ~570–470 ka time span, hardly envisaged from proximal successions. Nevertheless, the scarcity of literature data for the Middle Pleistocene volcanic activity of Italian volcanic districts, specifically for Roccamonfina, suggests that more studies focusing on a complete glass characterization of near-vent volcanic products are necessary to allow precise correlations between distal tephra and their proximal equivalents. Conscious of these limitations, instead of proposing a definitive correlation of some Acerno tephra layers with specific volcanic events, we aim at building a comprehensive geochemical database for future investigations into the Middle Pleistocene tephra framework of the Mediterranean area.

CG2 - Colli Albani - The A8, A13 and A19 tephra of CG2 can be unquestionably ascribed to some explosive events of the Colli Albani district, based on stratigraphic constraints and their peculiar major-, trace elements and Sr–Nd isotopic compositions. These tephra layers are widely distributed in Italian tephrostratigraphic archives.

CG3 - Pontian islands and the Neapolitan Volcanic Area - Finally, the tephra belonging the CG3 can be attributed to an ancient activity, belonging to the Pontian islands and the Neapolitan Volcanic Area, which has experienced explosive activity during the MIS 14–13, thus meaningfully antedating the beginning of volcanic activity in the area.

As far as the methodological approach is concerned, if on the one hand our study confirms the great potential of the central Mediterranean region for the development and application of the tephrochronology to Quaternary sciences and volcanology, on the other hand it also reveals how the current paucity of data available for the proximal volcanic sources represents a great limit for the full exploitation of this tool. Our multi-methodological approach, integrating stratigraphic position, age, major- and trace element and isotopic compositions of the tephra, also highlights the scarce reliability of some proposed correlations that were based on one or a few of these parameters. With this regard, our study also provides further evidence of how the combined use of radiogenic isotopes and major-trace element contents can provide strength to tephrostratigraphy, allowing volcanic source or even individual units to be more reliably identified than using the major and trace elements alone. Therefore, despite the present limitations, the results of this study provide a chronologically well-constrained geochemical database that will be useful for future investigations on tephra in the Mediterranean area, and which will allow correlating tephra layers of unknown origin to the events recognized in the Acerno basin and possibly to their volcanic source.

CRediT authorship contribution statement

C. Pelullo: Writing – original draft, Visualization, Software, Methodology, Formal analysis, Data curation. **I. Arienzo:** Writing – review & editing, Resources, Investigation. **M. D'Antonio:** Writing – review & editing, Validation, Supervision, Resources, Project administration, Investigation, Funding acquisition, Conceptualization. **B. Giaccio:** Writing – review & editing, Visualization, Methodology, Funding acquisition. **R.S. Iovine:** Writing – review & editing, Resources, Investigation. **N. Leicher:** Writing – review & editing, Visualization, Software, Methodology. **D.M. Palladino:** Writing – review & editing, Validation. **M. Petrelli:** Writing – review & editing, Resources, Investigation. **P. Petrosino:** Writing – review & editing, Resources, Investigation, Visualization, Supervision, Methodology. **E. Russo Ermolli:** Writing – review & editing, Methodology. **G. Sottili:** Writing – review & editing, Validation. **F. Totaro:** Writing – review & editing, Resources, Investigation. **G. Zanchetta:** Writing – review & editing, Project administration, Funding acquisition.

Declaration of competing interest

The authors declare that they have no known competing financial interests or personal relationships that could have appeared to influence the work reported in this paper.

Data availability

The original data produced in the frame of the present research are shared in Supplementary Material.

Acknowledgements

This research was part of the Project PRIN 2017 "FUTURE" (No. 20177TKBXZ_004) funded to G.Z., M.D., B.G. and D.P. by Italian

Ministry of University and Research (MUR). The INGV-OV laboratories have been financially supported by the EPOS Research Infrastructure through the contribution of the MUR. The authors wish to gratefully thank the reviewer Mathilde Bablon whose valuable suggestions deeply improved the final version of the paper.

Appendix A. Supplementary data

Supplementary data to this article can be found online at https://doi.org/10.1016/j.qsa.2024.100186.

References

Abbott, P.M., Jensen, B.J.L., Lowe, D.J., Suzuki, T., Veres, D., 2020. Crossing new frontiers: extending tephrochronology as a global geoscientific research tool. J. Quat. Sci. 35, 1–8.

Andronico, D., Cioni, R., 2002. Contrasting styles of Mount Vesuvius activity in the period between the Avellino and Pompeii Plinian eruptions, and some implications for assessment of future hazards. Bull. Volcanol. 64, 372–391.

Arienzo, I., Carandente, A., Di Renzo, V., Belviso, P., Civetta, L., D'Antonio, M., Orsi, G., 2013. Sr and Nd isotope analysis at the radiogenic isotope laboratory of the Istituto Nazionale di Geofisica e Vulcanologia, sezione di Napoli-Osservatorio Vesuviano. Rapp. Tec. INGV 260, 1–18. https://editoria.ingv.it/archivio_pdf/rapporti/259/pdf/rapporti_260.pdf.

Arienzo, I., Civetta, L., Heumann, A., Wörner, G., Orsi, G., 2009. Isotopic evidence for open system processes within the Campanian Ignimbrite (Campi Flegrei–Italy) magma chamber. Bull. Volcanol. 71, 285–300.

Arienzo, I., D'Antonio, M., Di Renzo, V., Tonarini, S., Minolfi, G., Orsi, G., Carandente, A., Belviso, P., Civetta, L., 2015. Isotopic microanalysis sheds light on the magmatic endmembers feeding volcanic eruptions: the Astroni 6 case study (Campi Flegrei, Italy). J. Volcanol. Geoth. Res. 304, 24–37.

Arienzo, I., Heumann, A., Wörner, G., Civetta, L., Orsi, G., 2011. Processes and timescales of magma evolution prior to the Campanian Ignimbrite eruption (Campi Flegrei, Italy). Earth Planet. Sci. Lett. 306, 217–228.

Arienzo, I., Mazzeo, F.C., Moretti, R., Cavallo, A., D'Antonio, M., 2016. Open-system magma evolution and fluid transfer at Campi Flegrei caldera (Southern Italy) during the past 5 ka as revealed by geochemical and isotopic data: the example of the Nisida eruption. Chem. Geol. 427, 109–124.

Aulinas, M., Civetta, L., Di Vito, M., Orsi, G., Gimeno, D., Férnandez-Turiel, J., 2008. The "Pomici di Mercato" Plinian eruption of Somma-Vesuvius: magma chamber processes and eruption dynamics. Bull. Volcanol. 70, 825–840.

Ayuso, R.A., De Vivo, B., Rolandi, G., Seal II, R.R., Paone, A., 1998. Geochemical and isotopic (Nd–Pb–Sr–O) variations bearing on the genesis of volcanic rocks from Vesuvius, Italy. J. Volcanol. Geoth. Res. 82, 53–78.

Avanzinelli, R., Elliott, T., Tommasini, S., Conticelli, S., 2008. Constraints on the genesis of the potassium-rich Italian volcanics from U/Th disequilibrium. J. Petrol. 49, 195–223.

Avanzinelli, R., Casalini, M., Elliott, T., Conticelli, S., 2018. Carbon fluxes from subducted carbonates revealed by uranium excess at Mount Vesuvius, Italy. Geology 46 (3), 259–262.

Ballini, A., Frullani, A., Mezzetti, F., 1989. La formazione piroclastica del Tufo Trachitico Bianco («White Trachytic Tuff»-WTT Auctorum) del vulcano di Roccamonfina. Boll. GNV 2, 557–574.

Barberi, F., Borsi, S., Ferrara, G., Innocenti, F., 1969. Strontium isotopic composition of some recent basic volcanites of the Southern Tyrrhenian Sea and Sicily Channel. Contrib. Mineral. Petrol. 23, 157–172.

Beccaluva, L., Di Girolamo, P., Serri, G., 1991. Petrogenesis and tectonic setting of the Roman volcanic Province, Italy. Lithos 26, 191–221.

Belkin, H.E., Kilburn, C.R., De Vivo, B., 1993. Chemistry of the Lavas and Tephra from the Recent (AD 1631-1944) Vesuvius (Italy) Volcanic Activity. US Department of the Interior, US Geological Survey Reston, VA, USA.

Bellucci, F., Lirer, L., Munno, R., 1999. Geology of Ponza, Ventotene and Santo Stefano islands (with a 1: 15,000 scale geological map). Acta Vulcanol. 11, 197–222.

Blaauw, M., Christen, J.A., 2011. Flexible paleoclimate age-depth models using an autoregressive gamma process. Bayesian Anal. 6 (3), 457–474.

Boari, E., Avanzinelli, R., Melluso, L., Giordano, G., Mattei, M., De Benedetti, A.A., Morra, V., Conticelli, S., 2009. Isotope geochemistry (Sr–Nd–Pb) and petrogenesis of leucite-bearing volcanic rocks from "Colli Albani" volcano, Roman Magmatic Province, Central Italy: inferences on volcano evolution and magma genesis. Bull. Volcanol. 71, 977–1005.

Boncio, P., Auciello, E., Amato, V., Aucelli, P., Petrosino, P., Tangari, A.C., Jicha, B.R., 2022. Late Quaternary faulting in the southern Matese (Italy): implications for earthquake potential and slip rate variability in the southern Apennines. Solid Earth 13, 553–582.

Bourne, A.J., Lowe, J., Trincardi, F., Asioli, A., Blockley, S., Wulf, S., Matthews, I., Piva, A., Vigliotti, L., 2010. Distal tephra record for the last ca 105,000 years from core PRAD 1-2 in the central Adriatic Sea: implications for marine tephrostratigraphy. Quat. Sci. Rev. 29, 3079–3094.

Bourne, A.J., Cook, E., Abbott, P.M., Seierstad, I.K., Steffensen, J.P., Svensson, A., Fischer, H., Schüpbach, S., Davies, S.M., 2015. A tephra lattice for Greenland and a reconstruction of volcanic events spanning 25–45 ka b2k. Quat. Sci. Rev. 118, 122–141.

Branca, S., Cinquegrani, A., Cioni, R., Conte, A.M., Conticelli, S., De Astis, G., de Vita, S., De Rosa, R., Di Vito, M.A., Donato, P., Forni, F., Francalanci, L., Gaeta, M., Giaccio, B., Giordano, G., Giuffrida, M., Isaia, R., Lucchi, F., Marra, F., Massaro, S., Nicotra, E., Palladino, D.M., Perinelli, C., Petrosino, P., Pistolesi, M., Romagnoli, C., Rotolo, S., Sottili, G., Sulpizio, R., Tranne, C.A., Viccaro, M., 2023. The Italian Quaternary volcanism. Alp. Mediterr. Quat. 36, 221–284.

Brown, R.J., Civetta, L., Arienzo, I., D'Antonio, M., Moretti, R., Orsi, G., Tomlinson, E.L., Albert, P.G., Menzies, M.A., 2014. Geochemical and isotopic insights into the assembly, evolution and disruption of a magmatic plumbing system before and after a cataclysmic caldera-collapse eruption at Ischia volcano (Italy). Contrib. Mineral. Petrol. 168, 1–23.

Buono, G., Pappalardo, L., Harris, C., Edwards, B.R., Petrosino, P., 2020. Magmatic stoping during the caldera-forming Pomici di Base eruption (Somma-Vesuvius, Italy) as a fuel of eruption explosivity. Lithos 370–371, 105628. https://doi.org/10.1016/j.lithos.2020.105628.

Cadoux, A., Blichert-Toft, J., Pinti, D.L., Albarède, F., 2007. A unique lower mantle source for Southern Italy volcanics. Earth Planet. Sci. Lett. 259, 227–238.

Cadoux, A., Pinti, D.L., Aznar, C., Chiesa, S., Gillot, P.Y., 2005. New chronological and geochemical constraints on the genesis and geological evolution of Ponza and Palmarola volcanic islands (Tyrrhenian Sea, Italy). Lithos 81, 121–151.

Capaldi, G., Cinque, A., Romano, P., 1988. Ricostruzione di sequenze morfoevolutive nei Picentini meridionali (Campania, Appennino meridionale). Geogr. Fis. Din. Quaternaria 1, 207–222 (in Italian).

Caprarelli, G., Togashi, S., De Vivo, B., 1993. Preliminary Sr and Nd isotopic data for recent lavas from Vesuvius volcano. J. Volcanol. Geoth. Res. 58, 377–381.

Casalini, M., Avanzinelli, R., Heumann, A., de Vita, S., Sansivero, F., Conticelli, S., Tommasini, S., 2017. Geochemical and radiogenic isotope probes of Ischia volcano, Southern Italy: constraints on magma chamber dynamics and residence time. Am. Mineral. 102, 262–274.

Cioni, R., Civetta, L., Marianelli, P., Métrich, N., Santacroce, R., Sbrana, A., 1995. Compositional layering and syn-eruptive mixing of a periodically refilled shallow magma chamber: the AD 79 Plinian eruption of Vesuvius. J. Petrol. 36, 739–776.

Civetta, L., Gallo, G., Orsi, G., 1991. Sr-and Nd-isotope and trace-element constraints on the chemical evolution of the magmatic system of Ischia (Italy) in the last 55 ka. J. Volcanol. Geoth. Res. 46, 213–230.

Civetta, L., Orsi, G., Pappalardo, L., Fisher, R.V., Heiken, G., Ort, M., 1997. Geochemical zoning, mingling, eruptive dynamics and depositional processes—the Campanian Ignimbrite, Campi Flegrei caldera, Italy. J. Volcanol. Geoth. Res. 75, 183–219.

Civetta, L., Santacroce, R., 1992. Steady-state magma supply in the last 3400 years of Vesuvius activity. Acta Vulcanol. 2, 147–159.

Conte, A., Dolfi, D., 2002. Petrological and geochemical characteristics of Plio-Pleistocene volcanics from Ponza Island (Tyrrhenian sea, Italy). Mineral. Petrol. 74, 75–94.

Conte, A., Perinelli, C., Bianchini, G., Natali, C., Martorelli, E., Chiocci, F., 2016. New insights on the petrology of submarine volcanics from the Western Pontine archipelago (Tyrrhenian sea, Italy). J. Volcanol. Geoth. Res. 327, 223–239.

Conte, A., Perinelli, C., Bosman, A., Castorina, F., 2020. Tectonics, dynamics, and Plio-Pleistocene magmatism in the Central Tyrrhenian Sea: insights from the submarine transitional basalts of the Ventotene volcanic ridge (Pontine Islands, Italy). Geochem. Geophys. Geosys. 21, e2020GC009346 https://doi.org/10.1029/2020GC009346.

Conticelli, S., Carlson, R.W., Widom, E., Serri, G., 2007. Chemical and isotopic composition (Os, Pb, Nd, and Sr) of Neogene to Quaternary calc-alkalic, shoshonitic, and ultrapotassic mafic rocks from the Italian peninsula: inferences on the nature of their mantle sources. In: Beccaluva, L., Bianchini, G., Wilson, M. (Eds.), Cenozoic Volcanism in the Mediterranean Area, vol. 418. Geol. Soc. Am. Spec. Paper, pp. 171–202.

Conticelli, S., D'Antonio, M., Pinarelli, L., Civetta, L., 2002. Source contamination and mantle heterogeneity in the genesis of Italian potassic and ultrapotassic volcanic rocks: Sr–Nd–Pb isotope data from Roman Province and Southern Tuscany. Mineral. Petrol. 74, 189–222.

Conticelli, S., Francalanci, L., Manetti, P., Cioni, R., Sbrana, A., 1997. Petrology and geochemistry of the ultrapotassic rocks from the Sabatini Volcanic District, central Italy: the role of evolutionary processes in the genesis of variably enriched alkaline magmas. J. Volcanol. Geoth. Res. 75, 107–136.

Conticelli, S., Marchionni, S., Rosa, D., Giordano, G., Boari, E., Avanzinelli, R., 2009. Shoshonite and sub-alkaline magmas from an ultrapotassic volcano: Sr–Nd–Pb isotope data on the Roccamonfina volcanic rocks, Roman Magmatic Province, Southern Italy. Contrib. Mineral. Petrol. 157, 41–63.

Cortini, M., Hermes, O.D., 1981. Sr isotopic evidence for a multi-source origin of the potassic magmas in the Neapolitan area (S. Italy). Contrib. Mineral. Petrol. 77, 47–55.

Crisci, G., De Francesco, A., Mazzuoli, R., Poli, G., Stanzione, D., 1989. Geochemistry of recent volcanics of Ischia Island, Italy: evidences for fractional crystallization and magma mixing. Chem. Geol. 78, 15–33.

D'Antonio, M., Civetta, L., Di Girolamo, P., 1999a. Mantle source heterogeneity in the Campanian Region (South Italy) as inferred from geochemical and isotopic features of mafic volcanic rocks with shoshonitic affinity. Mineral. Petrol. 67, 163–192.

D'Antonio, M., Civetta, L., Orsi, G., Pappalardo, L., Piochi, M., Carandente, A., de Vita, S., Di Vito, M.A., Isaia, R., 1999b. The present state of the magmatic system of the Campi Flegrei caldera based on a reconstruction of its behavior in the past 12 ka. J. Volcanol. Geoth. Res. 91, 247–268.

D'Antonio, M., Di Girolamo, P., 1994. Petrological and geochemical study of mafic shoshonitic volcanics from Procida-Vivara and Ventotene islands (Campanian region, south Italy). Acta Vulcanol. 5, 69–80.

D'Antonio, M., Mariconte, R., Arienzo, I., Mazzeo, F.C., Carandente, A., Perugini, D., Petrelli, M., Corselli, C., Orsi, G., Principato, M., 2016. Combined Sr-Nd isotopic and geochemical fingerprinting as a tool for identifying tephra layers: application to deep-sea cores from Eastern Mediterranean Sea. Chem. Geol. 443, 121–136.

D'Antonio, M., Tonarini, S., Arienzo, I., Civetta, L., Dallai, L., Moretti, R., Orsi, G., Andria, M., Trecalli, A., 2013. Mantle and crustal processes in the magmatism of the Campania region: inferences from mineralogy, geochemistry, and Sr–Nd–O isotopes of young hybrid volcanics of the Ischia island (South Italy). Contrib. Mineral. Petrol. 165, 1173–1194.

D'Antonio, M., Tonarini, S., Arienzo, I., Civetta, L., Di Renzo, V., 2007. Components and processes in the magma genesis of the Phlegrean Volcanic District, southern Italy. In: Beccaluva, L., Bianchini, G., Wilson, M. (Eds.), Cenozoic Volcanism in the Mediterranean Area, vol. 418. Geol. Soc. Am. Sp. Pap, Boulder, CO, USA, pp. 203–220.

D'Antonio, M., Tilton, G.R., Civetta, L., 1996. Petrogenesis of Italian alkaline lavas deduced from Pb-Sr-Nd isotope relationships. In: Basu, A., Hart, S.R. (Eds.), Earth Processes: Reading the Isotopic Code, vol. 95. Am. Geophys. Un. Monograph Series, pp. 253–267. https://doi.org/10.1029/GM095p0253.

Davies, S.M., 2015. Cryptotephras: the revolution in correlation and precision dating. J. Quat. Sci. 30, 114–130.

De Rita, D., Giordano, G., 1996. Volcanological and structural evolution of Roccamonfina volcano (Italy): origin of the summit caldera. Geol. Soc. Lond. Spec. Publ. 110, 209–224.

de Vita, S., Orsi, G., Civetta, L., Carandente, A., D'Antonio, M., Deino, A., Di Cesare, T., Di Vito, M., Fisher, R., Isaia, R., 1999. The Agnano–Monte Spina eruption (4100 years BP) in the restless Campi Flegrei caldera (Italy). J. Volcanol. Geoth. Res. 91, 269–301.

Del Bello, E., Mollo, S., Scarlato, P., von Quadt, A., Forni, F., Bachmann, O., 2014. New petrological constraints on the last eruptive phase of the Sabatini Volcanic District (central Italy): clues from mineralogy, geochemistry, and Sr–Nd isotopes. Lithos 205, 28–38.

Di Girolamo, P., Melluso, L., Morra, V., 1991. Magmatic activity northeast of Roccamonfina volcano (Southern Italy): petrology, geochemistry and relationships with Campanian volcanics. N. Jahrb. Mineral. Abh. 163, 271–289.

Di Girolamo, P., Melluso, L., Morra, V., Secchi, F., 1995. Evidence of interaction between mafic and intermediate magmas in the youngest activity phase of activity at Ischia Island (Italy). Period. Mineral. 64, 393–411.

Di Renzo, V., Di Vito, M., Arienzo, I., Carandente, A., Civetta, L., D'Antonio, M., Giordano, F., Orsi, G., Tonarini, S., 2007. Magmatic history of Somma–Vesuvius on the basis of new geochemical and isotopic data from a deep borehole (Camaldoli della Torre). J. Petrol. 48, 753–784.

Di Renzo, V., Arienzo, I., Civetta, L., D'Antonio, M., Tonarini, S., Di Vito, M.A., Orsi, G., 2011. The magmatic feeding system of the Campi Flegrei caldera: architecture and temporal evolution. Chem. Geol. 281, 227–234.

Di Renzo, V., Pelullo, C., Arienzo, I., Civetta, L., Petrosino, P., D'Antonio, M., 2022. Geochemical and Sr-isotopic study of clinopyroxenes from Somma-Vesuvius Lavas: inferences for magmatic processes and eruptive behavior. Minerals 12 (9), 1114. https://doi.org/10.3390/min12091114.

Di Rita, F., Sottili, G., 2019. Pollen analysis and tephrochronology of a MIS 13 lacustrine succession from eastern Sabatini volcanic district (Rignano Flaminio, central Italy). Quat. Sci. Rev. 204, 78–93.

Di Salvo, S., Avanzinelli, R., Isaia, R., Zanetti, A., Druitt, T., Francalanci, L., 2020. Crystal-mush reactivation by magma recharge: evidence from the Campanian Ignimbrite activity, Campi Flegrei volcanic field, Italy. Lithos 376, 105780. https://doi.org/10.1016/j.lithos.2020.105780.

Di Vito, M.A., Arienzo, I., Braia, G., Civetta, L., D'Antonio, M., Di Renzo, V., Orsi, G., 2011. The Averno 2 fissure eruption: a recent small-size explosive event at the Campi Flegrei Caldera (Italy). Bull. Volcanol. 73, 295–320.

Donders, T., Panagiotopoulos, K., Koutsodendris, A., Bertini, A., Mercuri, A.M., Masi, A., Combourieu-Nebout, N., Joannin, S., Kouli, K., Kousis, I., Peyron, O., Torri, P., Florenzano, A., Franke, A., Wagner, B., Sadori, L., 2021. 1.36 million years of Mediterranean forest refugium dynamics in response to glacial-interglacial cycle strength. Proc. Natl. Acad. Sci. USA 118, e2026111118. https://doi.org/10.1073/pnas.2026111118, 2021.

D'Oriano, C., Poggianti, E., Bertagnini, A., Cioni, R., Landi, P., Polacci, M., Rosi, M., 2005. Changes in eruptive style during the AD 1538 Monte Nuovo eruption (Phlegrean Fields, Italy): the role of syn-eruptive crystallization. Bull. Volcanol. 67, 601–621.

Favre, E., Escarguel, G., Suc, J.P., Vidal, G., Thévenod, L., 2008. A contribution to deciphering the meaning of AP/NAP with respect to vegetation cover. Rev. Palaeobot. Palynol. 148, 13–35.

Fedele, L., Zanetti, A., Morra, V., Lustrino, M., Melluso, L., Vannucci, R., 2009. Clinopyroxene/liquid trace element partitioning in natural trachyte–trachyphonolite systems: insights from Campi Flegrei (southern Italy). Contrib. Mineral. Petrol. 158, 337–356.

Forni, F., Bachmann, O., Mollo, S., De Astis, G., Gelman, S.E., Ellis, B.S., 2016. The origin of a zoned ignimbrite: insights into the Campanian Ignimbrite magma chamber (Campi Flegrei, Italy). Earth Planet. Sci. Lett. 449, 259–271.

Forni, F., Degruyter, W., Bachmann, O., De Astis, G., Mollo, S., 2018. Long-term magmatic evolution reveals the beginning of a new caldera cycle at Campi Flegrei. Sci. Adv. 4, eaat9401 https://doi.org/10.1126/sciadv.aat9401.

Fourmentraux, C., Métrich, N., Bertagnini, A., Rosi, M., 2012. Crystal fractionation, magma step ascent, and syn-eruptive mingling: the Averno 2 eruption (Phlegraean Fields, Italy). Contrib. Mineral. Petrol. 163, 1121–1137.

Gaeta, M., Bonechi, B., Marra, F., Perinelli, C., 2021. Uncommon K-foiditic magmas: the case study of Tufo del Palatino (Colli Albani Volcanic District, Italy). Lithos 396–397, 106239. https://doi.org/10.1016/j.lithos.2021.106239.

Gaeta, M., Freda, C., Christensen, J.N., Dallai, L., Marra, F., Karner, D.B., Scarlato, P., 2006. Time-dependent geochemistry of clinopyroxene from the Alban Hills (Central Italy): clues to the source and evolution of ultrapotassic magmas. Lithos 86, 330–346.

Gaeta, M., Freda, C., Marra, F., Arienzo, I., Gozzi, F., Jicha, B., Di Rocco, T., 2016. Paleozoic metasomatism at the origin of Mediterranean ultrapotassic magmas: constraints from time-dependent geochemistry of Colli Albani volcanic products (Central Italy). Lithos 244, 151–164.

Gaeta, M., Freda, C., Marra, F., Di Rocco, T., Gozzi, F., Arienzo, I., Giaccio, B., Scarlato, P., 2011. Petrology of the most recent ultrapotassic magmas from the Roman Province (Central Italy). Lithos 127, 298–308.

Galli, P., Giaccio, B., Messina, P., Peronace, E., Amato, V., Naso, G., Nomade, S., Pereira, A., Piscitelli, S., Bellanova, J., 2017. Middle to Late Pleistocene activity of the northern Matese fault system (southern Apennines, Italy). Tectonophysics 699, 61–81.

Gasperini, D., Blichert-Toft, J., Bosch, D., Del Moro, A., Macera, P., Albarède, F., 2002. Upwelling of deep mantle material through a plate window: evidence from the geochemistry of Italian basaltic volcanics. J. Geophys. Res. Solid Earth 107 (B12), 2367. https://doi:10.1029/2001JB000418.

Giaccio, B., Arienzo, I., Sottili, G., Castorina, F., Gaeta, M., Nomade, S., Galli, P., Messina, P., 2013a. Isotopic (Sr–Nd) and major element fingerprinting of distal tephras: an application to the Middle-Late Pleistocene markers from the Colli Albani volcano, central Italy. Quat. Sci. Rev. 67, 190–206.

Giaccio, B., Castorina, F., Nomade, S., Scardia, G., Voltaggio, M., Sagnotti, L., 2013b. Revised chronology of the Sulmona lacustrine succession, central Italy. J. Quat. Sci. 28, 545–551.

Giaccio, B., Galli, P., Messina, P., Peronace, E., Scardia, G., Sottili, G., Sposato, A., Chiarini, E., Jicha, B., Silvestri, S., 2012. Fault and basin depocentre migration over the last 2 Ma in the L'Aquila 2009 earthquake region, central Italian Apennines. Quat. Sci. Rev. 56, 69–88.

Giaccio, B., Galli, P., Peronace, E., Arienzo, I., Nomade, S., Cavinato, G.P., Mancini, M., Messina, P., Sottili, G., 2014. A 560–440 ka tephra record from the Mercure Basin, southern Italy: volcanological and tephrostratigraphic implications. J. Quat. Sci. 29, 232–248.

Giaccio, B., Hajdas, I., Isaia, R., Deino, A., Nomade, S., 2017a. High-precision ^{14}C and $^{40}Ar/^{39}Ar$ dating of the Campanian Ignimbrite (Y-5) reconciles the timescales of climatic-cultural processes at 40 ka. Sci. Rep. 7, 45940 https://doi.org/10.1038/srep45940.

Giaccio, B., Niespolo, E.M., Pereira, A., Nomade, S., Renne, P.R., Albert, P.G., Arienzo, I., Regattieri, E., Wagner, B., Zanchetta, G., Gaeta, M., Galli, P., Mannella, G., Peronace, E., Sottili, G., Florindo, F., Leicher, N., Marra, F., Tomlinson, E.L., 2017b. First integrated tephrochronological record for the last ~190 kyr from the Fucino Quaternary lacustrine succession, central Italy. Quat. Sci. Rev. 158, 211–234.

Giaccio, B., Leicher, N., Mannella, G., Monaco, L., Regattieri, E., Wagner, B., Zanchetta, G., Gaeta, M., Marra, F., Nomade, S., 2019. Extending the tephra and palaeoenvironmental record of the Central Mediterranean back to 430 ka: a new core from Fucino Basin, central Italy. Quat. Sci. Rev. 225, 106003 https://doi.org/10.1016/j.quascirev.2019.106003.

Giaccio, B., Messina, P., Sposato, A., Voltaggio, M., Zanchetta, G., Galadini, F., Gori, S., Santacroce, R., 2009. Tephra layers from Holocene lake sediments of the Sulmona Basin, central Italy: implications for volcanic activity in Peninsular Italy and tephrostratigraphy in the central Mediterranean area. Quat. Sci. Rev. 28, 2710–2733.

Giaccio, B., Regattieri, E., Zanchetta, G., Wagner, B., Galli, P., Mannella, G., Niespolo, E., Peronace, E., Renne, P., Nomade, S., 2015. A key continental archive for the last 2 Ma of climatic history of the central Mediterranean region: a pilot drilling in the Fucino Basin, central Italy. Sci. Drill. 20, 13–19.

Giannetti, B., Ellam, R., 1994. The primitive lavas of Rocccamonfina volcano, Roman region, Italy: new constraints on melting processes and source mineralogy. Contrib. Mineral. Petrol. 116, 21–31.

Giordano, G., De Benedetti, A., Diana, A., Diano, G., Gaudioso, F., Marasco, F., Miceli, M., Mollo, S., Cas, R.A.F., Funiciello, R., 2006. The Colli Albani mafic caldera (Roma, Italy): stratigraphy, structure and petrology. J. Volcanol. Geoth. Res. 155, 49–80.

Goldstein, S.L., Deines, P., Oelkers, E.H., Rudnick, R.L., Walter, L.M., 2003. Standards for publication of isotope ratio and chemical data in Chemical Geology. Chem. Geol. 202, 1–4.

Hawkesworth, C., Vollmer, R., 1979. Crustal contamination versus enriched mantle: $^{143}Nd/^{144}Nd$ and $^{87}Sr/^{86}Sr$ evidence from the Italian volcanics. Contrib. Mineral. Petrol. 69, 151–165.

Insinga, D., Tamburrino, S., Lirer, F., Vezzoli, L., Barra, M., De Lange, G., Tiepolo, M., Vallefuoco, M., Mazzola, S., Sprovieri, M., 2014. Tephrochronology of the astronomically-tuned KC01B deep-sea core, Ionian Sea: insights into the explosive activity of the Central Mediterranean area during the last 200 ka. Quat. Sci. Rev. 85, 63–84.

Iovine, R.S., Mazzeo, F.C., Arienzo, I., D'Antonio, M., Wörner, G., Civetta, L., Pastore, Z., Orsi, G., 2017. Source and magmatic evolution inferred from geochemical and Sr-O-isotope data on hybrid lavas of Arso, the last eruption at Ischia island (Italy; 1302 AD). J. Volcanol. Geoth. Res. 331, 1–15.

Joron, J., Metrich, N., Rosi, M., Santacroce, R., Sbrana, A., 1987. Chemistry and petrography. In: "Somma-Vesuvius" CNR, Quaderni de La Ricerca Scientifica, vol. 114. Progetto Finalizzato Geodinamica, Monografie Finali, pp. 105–171.

Karner, D.B., Marra, F., Renne, P.R., 2001. The history of the Monti Sabatini and Alban Hills volcanoes: groundwork for assessing volcanic-tectonic hazards for Rome. J. Volcanol. Geoth. Res. 107, 185–219.
Keller, J., Ryan, W., Ninkovich, D., Altherr, R., 1978. Explosive volcanic activity in the Mediterranean over the past 200,000 yr as recorded in deep-sea sediments. Geol. Soc. Am. Bull. 89, 591–604.
Koornneef, J.M., Nikogosian, I., van Bergen, M.J., Smeets, R., Bouman, C., Davies, G.R., 2015. TIMS analysis of Sr and Nd isotopes in melt inclusions from Italian potassium-rich lavas using prototype 10^{13} Ω amplifiers. Chem. Geol. 397, 14–23.
Kousis, I., Koutsodendris, A., Peyron, O., Leicher, N., Francke, A., Wagner, B., Giaccio, B., Knipping, M., Pross, J., 2018. Centennial-scale vegetation dynamics and climate variability in SE Europe during Marine Isotope Stage 11 based on a pollen record from Lake Ohrid. Quat. Sci. Rev. 190, 20–38.
Lane, C.S., Lowe, D.J., Blockley, S.P., Suzuki, T., Smith, V.C., 2017. Advancing tephrochronology as a global dating tool: applications in volcanology, archaeology, and palaeoclimatic research. Quat. Geochronol. 40, 1–7.
Leicher, N., Giaccio, B., Pereira, A., Nomade, S., Monaco, L., Mannella, G., Galli, P., Peronance, E., Palladino, D.M., Sottili, G., 2023. Central Mediterranean tephrochronology between 313 and 366 ka: new insights from the Fucino palaeolake sediment succession. Boreas 52, 240–271. https://doi.org/10.1111/bor.12610.
Leicher, N., Giaccio, B., Zanchetta, G., Sulpizio, R., Albert, P.G., Tomlinson, E.L., Lagos, M., Francke, A., Wagner, B., 2021. Lake Ohrid's tephrochronological dataset reveals 1.36 Ma of Mediterranean explosive volcanic activity. Sci. Data 8, 231. https://doi.org/10.1038/s41597-021-01013-7.
Leicher, N., Giaccio, B., Zanchetta, G., Wagner, B., Francke, A., Palladino, D.M., Sulpizio, R., Albert, P.G., Tomlinson, E.L., 2019. Central Mediterranean explosive volcanism and tephrochronology during the last 630 ka based on the sediment record from Lake Ohrid. Quat. Sci. Rev. 226, 106021 https://doi.org/10.1016/j.quascirev.2019.106021.
Leicher, N., Zanchetta, G., Sulpizio, R., Giaccio, B., Wagner, B., Nomade, S., Francke, A., Del Carlo, P., 2016. First tephrostratigraphic results of the DEEP site record from Lake Ohrid (Macedonia and Albania). Biogeosciences 13, 2151–2178.
Le Maitre, R.W. (Ed.), 2002. Igneous Rocks. A Classification and Glossary of Terms. Recommendations of the International Union of Geological Sciences Subcommission on the Systematics of Igneous Rocks, Second ed. Cambridge University Press, Cambridge, New York, Melbourne, p. 1-236.
Lisiecki, L.E., Raymo, M.E., 2005. A Pliocene-Pleistocene stack of 57 globally distributed benthic $\delta^{18}O$ records. Paleoceanography 20, PA1003. https://doi.org/10.1029/2004PA001071.
Lowe, D.J., 2011. Tephrochronology and its application: a review. Quat. Geochronol. 6, 107–153.
Lowe, D.J., Hunt, J.B., 2001. A summary of terminology used in tephra-related studies. In: Juvigné, E.T., Raynal, J.-P. (Eds.), Tephras: Chronology, Archaeology. CDERAD Ed., Goudet, Les Dossiers de l'Archéo-Logis, vol. 1, pp. 17–22.
Lustrino, M., Marturano, A., Morra, V., Ricci, G., 2002. Volcanological and geochemical features of young pyroclastic levels (< 12 ka) in the urban area of Naples (S. Italy). Period. Mineral. 71, 241–253.
Lyubetskaya, T., Korenaga, J., 2007. Chemical composition of Earth's primitive mantle and its variance: 1. Method and results. J. Geophys. Res. Solid Earth 112, B03211. https://doi.org/10.1029/2005JB004223.
Marra, F., Costantini, L., Di Buduo, G., Florindo, F., Jicha, B., Monaco, L., Palladino, D. M., Sottili, G., 2019. Combined glacio-eustatic forcing and volcano-tectonic uplift: geomorphological and geochronological constraints on the Tiber River terraces in the eastern Vulsini Volcanic District (central Italy). Global Planet. Change 182, 103009. https://doi.org/10.1016/j.gloplacha.2019.103009.
Marra, F., Deocampo, D., Jackson, M., Ventura, G., 2011. The Alban Hills and Monti Sabatini volcanic products used in ancient Roman masonry (Italy): an integrated stratigraphic, archaeological, environmental and geochemical approach. Earth Sci. Rev. 108, 115–136.
Marra, F., Florindo, F., Jicha, B.R., 2017. $^{40}Ar/^{39}Ar$ dating of glacial termination VI: constraints on the duration of marine isotopic stage 13. Sci. Rep. 7, 8908. https://doi.org/10.1038/s41598-017-08614-6.
Marra, F., Jicha, B., Palladino, D.M., Gaeta, M., Costantini, L., Di Buduo, G.M., 2020. $^{40}Ar/^{39}Ar$ single crystal dates from pyroclastic deposits provide a detailed record of the 590–240 ka eruptive period at the Vulsini Volcanic District (central Italy). J. Volcanol. Geoth. Res. 398, 106904 https://doi.org/10.1016/j.jvolgeores.2020.106904.
Marra, F., Karner, D.B., Freda, C., Gaeta, M., Renne, P., 2009. Large mafic eruptions at Alban Hills Volcanic District (Central Italy): chronostratigraphy, petrography and eruptive behavior. J. Volcanol. Geoth. Res. 179, 217–232.
Marra, F., Sottili, G., Gaeta, M., Giaccio, B., Jicha, B., Masotta, M., Palladino, D.M., Deocampo, D., 2014. Major explosive activity in the Monti Sabatini Volcanic District (central Italy) over the 800–390 ka interval: geochronological–geochemical overview and tephrostratigraphic implications. Quat. Sci. Rev. 94, 74–101.
Martelli, M., Nuccio, P., Stuart, F., Burgess, R., Ellam, R., Italiano, F., 2004. Helium–strontium isotope constraints on mantle evolution beneath the Roman Comagmatic Province, Italy. Earth Planet. Sci. Lett. 224, 295–308.
Marturano, A., Aiello, G., Barra, D., Fedele, L., Grifa, C., Morra, V., Berg, R., Varone, A., 2009. Evidence for Holocenic uplift at Somma-Vesuvius. J. Volcanol. Geoth. Res. 184, 451–461.
Masotta, M., Gaeta, M., Gozzi, F., Marra, F., Palladino, D.M., Sottili, G., 2010. H_2O- and temperature-zoning in magma chambers: the example of the Tufo Giallo della Via Tiberina eruptions (Sabatini volcanic district, central Italy). Lithos 118, 119–130.
Melluso, L., Morra, V., Perrotta, A., Scarpati, C., Adabbo, M., 1995. The eruption of the Breccia Museo (Campi Flegrei, Italy): fractional crystallization processes in a shallow, zoned magma chamber and implications for the eruptive dynamics. J. Volcanol. Geoth. Res. 68, 325–339.
Monaco, L., Leicher, N., Palladino, D.M., Arienzo, I., Marra, F., Petrelli, M., Nomade, S., Pereira, A., Sottili, G., Conticelli, S., D'Antonio, M., Fabbrizio, A., Jicha, B.R., Mannella, G., Petrosino, P., Regattieri, E., Tzedakis, P.C., Wagner, B., Zanchetta, G., Giaccio, B., 2022a. The Fucino 250–170 ka tephra record: new insights on peri-Tyrrhenian explosive volcanism, central mediterranean tephrochronology, and timing of the MIS 8-6 climate variability. Quat. Sci. Rev. 296, 107797 https://doi.org/10.1016/j.quascirev.2022.107797.
Monaco, L., Palladino, D.M., Albert, P.G., Arienzo, I., Conticelli, S., Di Vito, M., Fabbrizio, A., D'Antonio, M., Isaia, R., Manning, C.J., Nomade, S., Pereira, A., Petrosino, P., Sottili, G., Sulpizio, R., Zanchetta, G., Giaccio, B., 2022b. Linking the Mediterranean MIS 5 tephra markers to Campi Flegrei (southern Italy) 109–92 ka explosive activity and refining the chronology of MIS 5c-d millennial-scale climate variability. Global Planet. Change 211, 103785. https://doi.org/10.1016/j.gloplacha.2022.103785.
Monaco, L., Palladino, D.M., Gaeta, M., Marra, F., Sottili, G., Leicher, N., Mannella, G., Nomade, S., Pereira, A., Regattieri, E., Wagner, B., Zanchetta, G., Albert, P.G., Arienzo, I., D'Antonio, M., Petrosino, P., Manning, C.J., Giaccio, B., 2021. Mediterranean tephrostratigraphy and peri-Tyrrhenian explosive activity revaluated in light of the 430-365 ka record from Fucino Basin (central Italy). Earth Sci. Rev. 220, 103706 https://doi.org/10.1016/j.earscirev.2021.103706.
Morabito, S., Petrosino, P., Milia, A., Sprovieri, M., Tamburrino, S., 2014. A multidisciplinary approach for reconstructing the stratigraphic framework of the last 40 ka in a bathyal area of the eastern Tyrrhenian Sea. Global Planet. Change 123, 121–138.
Munno, R., Petrosino, P., Romano, P., Russo Ermolli, E., Juvigné, É., 2001. A late Middle Pleistocene climatic cycle in southern Italy inferred from pollen analysis and tephrostratigraphy of the Acerno lacustrine succession. Géogr. Phys. Quaternaire 55, 87–99.
Nappi, G., Renzulli, A., Santi, P., 1987. An evolutionary model for the Paleobolsena and Bolsena volcanic complexes: a structural and petrographic study. Period. Mineral. 56, 241–267.
Nappi, G., Renzulli, A., Santi, P., Gillot, P.Y., 1995. Geological evolution and geochronology of the Vulsini volcanic district (Central Italy). Boll. Soc. Geol. Ital. 114, 599–613.
Niespolo, E.M., Rutte, D., Deino, A.L., Renne, P.R., 2017. Intercalibration and age of the Alder Creek sanidine $^{40}Ar/^{39}Ar$ standard. Quat. Geochronol. 39, 205–213.
Orsi, G., Civetta, L., D'Antonio, M., Di Girolamo, P., Piochi, M., 1995. Step-filling and development of a three-layer magma chamber: the Neapolitan Yellow Tuff case history. J. Volcanol. Geoth. Res. 67, 291–312.
Orsi, G., D'Antonio, M., de Vita, S., Gallo, G., 1992. The Neapolitan Yellow Tuff, a large-magnitude trachytic phreatoplinian eruption: eruptive dynamics, magma withdrawal and caldera collapse. J. Volcanol. Geoth. Res. 53, 275–287.
Pabst, S., Wörner, G., Civetta, L., Tesoro, R., 2008. Magma chamber evolution prior to the Campanian Ignimbrite and Neapolitan Yellow Tuff eruptions (Campi Flegrei, Italy). Bull. Volcanol. 70, 961–976.
Palladino, D.M., Gaeta, M., Marra, F., 2001. A large K-foiditic hydromagmatic eruption from the early activity of the Alban Hills Volcanic District, Italy. Bull. Volcanol. 63, 345–359.
Palladino, D.M., Simei, S., Sottili, G., Trigila, R., 2010. Integrated approach for the reconstruction of stratigraphy and geology of Quaternary volcanic terrains: an application to the Vulsini Volcanoes (central Italy). In: Groppelli, G., Viereck-Goette, L. (Eds.), Stratigraphy and Geology of Volcanic Areas, vol. 464. Geol. Soc. Am. Sp. Pap, Boulder, CO, USA, pp. 63–84.
Palladino, D.M., Gaeta, M., Giaccio, B., Sottili, G., 2014. On the anatomy of magma chamber and caldera collapse: the example of trachy-phonolitic explosive eruptions of the Roman Province (central Italy). J. Volcanol. Geoth. Res. 281, 12–26.
Paone, A., 2006. The geochemical evolution of the Mt. Somma-Vesuvius volcano. Mineral. Petrol. 87, 53–80.
Pappalardo, L., Civetta, L., D'Antonio, M., Deino, A., Di Vito, M., Orsi, G., Carandente, A., de Vita, S., Isaia, R., Piochi, M., 1999. Chemical and Sr-isotopical evolution of the phlegraean magmatic system before the Campanian Ignimbrite and the Neapolitan Yellow Tuff eruptions. J. Volcanol. Geoth. Res. 91, 141–166.
Pappalardo, L., Ottolini, L., Mastrolorenzo, G., 2008. The Campanian Ignimbrite (southern Italy) geochemical zoning: insight on the generation of a super-eruption from catastrophic differentiation and fast withdrawal. Contrib. Mineral. Petrol. 156, 1–26.
Pappalardo, L., Piochi, M., D'Antonio, M., Civetta, L., Petrini, R., 2002. Evidence for multi-stage magmatic evolution during the past 60 kyr at Campi Flegrei (Italy) deduced from Sr, Nd and Pb isotope data. J. Petrol. 43, 1415–1434.
Paterne, M., Guichard, F., Duplessy, J., Siani, G., Sulpizio, R., Labeyrie, J., 2008. A 90,000–200,000 yrs marine tephra record of Italian volcanic activity in the Central Mediterranean Sea. J. Volcanol. Geoth. Res. 177, 187–196.
Paterne, M., Guichard, F., Labeyrie, J., 1988. Explosive activity of the South Italian volcanoes during the past 80,000 years as determined by marine tephrochronology. J. Volcanol. Geoth. Res. 34, 153–172.
Paterne, M., Guichard, F., Labeyrie, J., Gillot, P., Duplessy, J.-C., 1986. Tyrrhenian Sea tephrochronology of the oxygen isotope record for the past 60,000 years. Mar. Geol. 72, 259–285.
Paul, B., Petrus, J., Savard, D., Woodhead, J., Hergt, J., Greig, A., Paton, C., Rayner, P., 2023. Time resolved trace element calibration strategies for LA-ICP-MS. J. Anal. At. Spectrom. 38, 1995–2006.
Peccerillo, A., 2017. Cenozoic volcanism in the Tyrrhenian Sea region. In: Nemeth, K. (Ed.), Advances in Volcanology, Second ed. Springer International Publishing, New York, pp. 1–399.

Pelullo, C., Cirillo, G., Iovine, R.S., Arienzo, I., Aulinas, M., Pappalardo, L., Petrosino, P., Fernandez-Turiel, J.L., D'Antonio, M., 2020. Geochemical and Sr–Nd isotopic features of the Zaro Volcanic Complex: insights on the magmatic processes triggering a small-scale prehistoric eruption at Ischia Island (South Italy). Int. J. Earth Sci. 109, 2829–2849.

Petrelli, M., Bizzarri, R., Morgavi, D., Baldanza, A., Perugini, D., 2017. Combining machine learning techniques, microanalyses and large geochemical datasets for tephrochronological studies in complex volcanic areas: new age constraints for the Pleistocene magmatism of central Italy. Quat. Geochronol. 40, 33–44.

Petrelli, M., Morgavi, D., Vetere, F.P., Perugini, D., 2016. Elemental imaging and petro-volcanological applications of an improved laser ablation inductively coupled quadrupole plasma mass spectrometry. Period. Mineral. 85, 25–39.

Petrosino, P., Arienzo, I., Mazzeo, F.C., Natale, J., Petrelli, M., Milia, A., Perugini, D., D'Antonio, M., 2019. The San Gregorio Magno lacustrine basin (Campania, southern Italy): improved characterization of the tephrostratigraphic markers based on trace elements and isotopic data. J. Quat. Sci. 34, 393–404.

Petrosino, P., Russo Ermolli, E., Donato, P., Jicha, B., Robustelli, G., Sardella, R., 2014a. Using tephrochronology and palynology to date the MIS 13 lacustrine sediments of the Mercure Basin (Southern Apennines–Italy). Ital. J. Geosci. 133, 169–186.

Petrosino, P., Jicha, B., Mazzeo, F.C., Ciaranfi, N., Girone, A., Maiorano, P., Marino, M., 2015. The Montalbano Jonico marine succession: an archive for distal tephra layers at the Early–Middle Pleistocene boundary in southern Italy. Quat. Int. 383, 89–103.

Petrosino, P., Jicha, B., Mazzeo, F.C., Russo Ermolli, E., 2014b. A high resolution tephrochronological record of MIS 14–12 in the Southern Apennines (Acerno Basin, Italy). J. Volcanol. Geoth. Res. 274, 34–50.

Petrosino, P., Morabito, S., Jicha, B.R., Milia, A., Sprovieri, M., Tamburrino, S., 2016. Multidisciplinary tephrochronological correlation of marker events in the eastern Tyrrhenian Sea between 48 and 105 ka. J. Volcanol. Geoth. Res. 315, 79–99.

Piochi, M., Ayuso, R.A., De Vivo, B., Somma, R., 2006. Crustal contamination and crystal entrapment during polybaric magma evolution at Mt. Somma–Vesuvius volcano, Italy: geochemical and Sr isotope evidence. Lithos 86, 303–329.

Piochi, M., Civetta, L., Orsi, G., 1999. Mingling in the magmatic system of Ischia (Italy) in the past 5 ka. Mineral. Petrol. 66, 227–258.

Poli, S., Chiesa, S., Gillot, P.-Y., Gregnanin, A., Guichard, F., 1987. Chemistry versus time in the volcanic complex of Ischia (Gulf of Naples, Italy): evidence of successive magmatic cycles. Contrib. Mineral. Petrol. 95, 322–335.

Porreca, M., Mattei, M., 2010. Tectonic and environmental evolution of Quaternary intramontane basins in Southern Apennines (Italy): insights from palaeomagnetic and rock magnetic investigations. Geophys. J. Int. 182, 682–698.

R Core Team, 2022. R: A Language and Environment for Statistical Computing. R Foundation for Statistical Computing, Vienna, Austria. www.R-project.org.

Regattieri, E., Giaccio, B., Galli, P., Nomade, S., Peronace, E., Messina, P., Sposato, A., Boschi, C., Gemelli, M., 2016. A multi-proxy record of MIS 11-12 deglaciation and glacial MIS 12 instability from the Sulmona Basin (central Italy). Quat. Sci. Rev. 132, 129–145.

Regattieri, E., Giaccio, B., Mannella, G., Zanchetta, G., Nomade, S., Tognarelli, A., Perchiazzi, N., Vogel, H., Boschi, C., Drysdale, R.N., 2019. Frequency and dynamics of millennial-scale variability during marine isotope stage 19: insights from the Sulmona basin (central Italy). Quat. Sci. Rev. 214, 28–43.

Regattieri, E., Giaccio, B., Zanchetta, G., Drysdale, R.N., Galli, P., Nomade, S., Peronace, E., Wulf, S., 2015. Hydrological variability over the Apennines during the Early Last Glacial precession minimum, as revealed by a stable isotope record from Sulmona basin, Central Italy. J. Quat. Sci. 30, 19–31.

Renne, P.R., Balco, G., Ludwig, K.R., Mundil, R., Min, K., 2011. Response to the comment by WH Schwarz et al. on "Joint determination of ^{40}K decay constants and ^{40}Ar*/^{40}K for the Fish Canyon sanidine standard, and improved accuracy for ^{40}Ar/^{39}Ar geochronology". Geochim Cosmochim. Acta 75, 5097–5100, 2010.

Rolandi, G., Bellucci, F., Heizler, M., Belkin, H., De Vivo, B., 2003. Tectonic controls on the genesis of ignimbrites from the Campanian Volcanic Zone, southern Italy. Mineral. Petrol. 79, 3–31.

Rouchon, V., Gillot, P., Quidelleur, X., Chiesa, S., Floris, B., 2008. Temporal evolution of the Roccamonfina volcanic complex (Pleistocene), Central Italy. J. Volcanol. Geoth. Res. 177, 500–514.

Russo Ermolli, E., 2000. Pollen analysis of the Acerno palaeo-lacustrine succession (Middle Pleistocene, southern Italy). Geol. Soc. Lond. Spec. Publ. 181, 151–159.

Salvador, A. (Ed.), 1994. International Stratigraphic Guide, second ed. Geological Society of America, Boulder.

Santacroce, R., Bertagnini, A., Civetta, L., Landi, P., Sbrana, A., 1993. Eruptive dynamics and petrogenetic processes in a very shallow magma reservoir: the 1906 eruption of Vesuvius. J. Petrol. 34, 383–425.

Santacroce, R., Cioni, R., Marianelli, P., Sbrana, A., Sulpizio, R., Zanchetta, G., Donahue, D.J., Joron, J.L., 2008. Age and whole rock–glass compositions of proximal pyroclastics from the major explosive eruptions of Somma-Vesuvius: a review as a tool for distal tephrostratigraphy. J. Volcanol. Geoth. Res. 177, 1–18.

Slejko, F.F., Petrini, R., Orsi, G., Piochi, M., Forte, C., 2004. Water speciation and Sr isotopic exchange during water–melt interaction: a combined NMR–TIMS study on the Cretaio Tephra (Ischia Island, south Italy). J. Volcanol. Geoth. Res. 133, 311–320.

Smith, V., Isaia, R., Pearce, N., 2011. Tephrostratigraphy and glass compositions of post-15 kyr Campi Flegrei eruptions: implications for eruption history and chronostratigraphic markers. Quat. Sci. Rev. 30, 3638–3660.

Somma, R., Ayuso, R., De Vivo, B., Rolandi, G., 2001. Major, trace element and isotope geochemistry (Sr-Nd-Pb) of interplinian magmas from Mt. Somma-Vesuvius (Southern Italy). Mineral. Petrol. 73, 121–143.

Sottili, G., Arienzo, I., Castorina, F., Gaeta, M., Giaccio, B., Marra, F., Palladino, D.M., 2019. Time-dependent Sr and Nd isotope variations during the evolution of the ultrapotassic Sabatini volcanic district (Roman Province, central Italy). Bull. Volcanol. 81, 1–19.

Sottili, G., Palladino, D.M., Zanon, V., 2004. Plinian activity during the early eruptive history of the Sabatini Volcanic District, Central Italy. J. Volcanol. Geoth. Res. 135, 361–379.

Sparice, D., Scarpati, C., Mazzeo, F.C., Petrosino, P., Arienzo, I., Gisbert, G., Petrelli, M., 2017. New proximal tephras at Somma-Vesuvius: evidences of a pre-caldera, large (?) explosive eruption. J. Volcanol. Geoth. Res. 335, 71–81.

Tamburrino, S., Insinga, D.D., Sprovieri, M., Petrosino, P., Tiepolo, M., 2012. Major and trace element characterization of tephra layers offshore Pantelleria Island: insights into the last 200 ka of volcanic activity and contribution to the Mediterranean tephrochronology. J. Quat. Sci. 27, 129–140.

Tomlinson, E.L., Albert, P.G., Wulf, S., Brown, R.J., Smith, V.C., Keller, J., Orsi, G., Bourne, A.J., Menzies, M.A., 2014. Age and geochemistry of tephra layers from Ischia, Italy: constraints from proximal-distal correlations with Lago Grande di Monticchio. J. Volcanol. Geoth. Res. 287, 22–39.

Tomlinson, E.L., Arienzo, I., Civetta, L., Wulf, S., Smith, V.C., Hardiman, M., Lane, C.S., Carandente, A., Orsi, G., Rosi, M., 2012. Geochemistry of the Phlegraean Fields (Italy) proximal sources for major Mediterranean tephras: implications for the dispersal of Plinian and co-ignimbritic components of explosive eruptions. Geochim. Cosmochim. Acta 93, 102–128.

Tomlinson, E.L., Smith, V.C., Albert, P.G., Aydar, E., Civetta, L., Cioni, R., Çubukçu, E., Gertisser, R., Isaia, R., Menzies, M.A., 2015. The major and trace element glass compositions of the productive Mediterranean volcanic sources: tools for correlating distal tephra layers in and around Europe. Quat. Sci. Rev. 118, 48–66.

Tonarini, S., D'Antonio, M., Di Vito, M.A., Orsi, G., Carandente, A., 2009. Geochemical and B–Sr–Nd isotopic evidence for mingling and mixing processes in the magmatic system that fed the Astroni volcano (4.1–3.8 ka) within the Campi Flegrei caldera (southern Italy). Lithos 107, 135–151.

Tonarini, S., Leeman, W., Civetta, L., D'Antonio, M., Ferrara, G., Necco, A., 2004. B/Nb and δ^{11}B systematics in the Phlegrean volcanic district, Italy. J. Volcanol. Geoth. Res. 133, 123–139.

Totaro, F., Insinga, D.D., Lirer, F., Margaritelli, G., Català i Caparrós, A., de la Fuente, M., Petrosino, P., 2022. The Late Pleistocene to Holocene tephra record of ND14Q site (southern Adriatic Sea): traceability and preservation of Neapolitan explosive products in the marine realm. J. Volcanol. Geoth. Res. 423, 107461 https://doi.org/10.1016/j.jvolgeores.2021.107461.

Turi, B., Taylor Jr, H.P., Ferrara, G., 1991. Comparisons of ^{18}O/^{16}O and ^{87}Sr/^{86}Sr in volcanic rocks from the Pontine Islands, M. Ernici, and Campania with other areas in Italy. In: Taylor, H.P., O'Neil, J.R., Kaplan, I.R. (Eds.), Stable Isotope Geochemistry: A Tribute to Samuel Epstein, vol. 3. Geochem. Soc. Spec. Publ., pp. 307–324

Vakhrameeva, P., Koutsodendris, A., Wulf, S., Portnyagin, M., Appelt, O., Ludwig, T., Trieloff, M., Pross, J., 2021. Land-sea correlations in the Eastern Mediterranean region over the past c. 800 kyr based on macro-and cryptotephras from ODP Site 964 (Ionian Basin). Quat. Sci. Rev. 255, 106811 https://doi.org/10.1016/j.quascirev.2021.106811.

Valente, E., Buscher, J.T., Jourdan, F., Petrosino, P., Reddy, S.M., Tavani, S., Corradetti, A., Ascione, A., 2019. Constraining mountain front tectonic activity in extensional setting from geomorphology and Quaternary stratigraphy: a case study from the Matese ridge, southern Apennines. Quat. Sci. Rev. 219, 47–67.

Vidal, C.M., Fontijn, K., Lane, C.S., Asrat, A., Barfod, D., Tomlinson, E.L., Piermattei, A., Hutchison, W., Tadesse, A.Z., Yirgu, G., 2022. Geochronology and glass geochemistry of major Pleistocene eruptions in the Main Ethiopian Rift: towards a regional tephrostratigraphy. Quat. Sci. Rev. 290, 107601 https://doi.org/10.1016/j.quascirev.2022.107601.

Villemant, B., Trigila, R., De Vivo, B., 1993. Geochemistry of Vesuvius volcanics during 1631–1944 period. J. Volcanol. Geoth. Res. 58, 291–313.

Voloschina, M., Pistolesi, M., Bertagnini, A., Métrich, N., Pompilio, M., Di Roberto, A., Di Salvo, S., Francalanci, L., Isaia, R., Cioni, R., 2018. Magmatic reactivation of the Campi Flegrei volcanic system: insights from the Baia–Fondi di Baia eruption. Bull. Volcanol. 80, 1–21.

Wagner, B., Vogel, H., Francke, A., Friedrich, T., Donders, T., Lacey, J.H., Leng, M.J., Regattieri, E., Sadori, L., Wilke, T., Zanchetta, G., Albrecht, C., Bertini, A., Combourieu-Nebout, N., Cvetkoska, A., Giaccio, B., Grazhdani, A., Hauffe, T., Holtvoeth, J., Joannin, S., Jovanovska, E., Just, J., Kouli, K., Kousis, I., Koutsodendris, A., Krastel, S., Lagos, M., Leicher, N., Levkov, Z., Lindhorst, K., Masi, A., Melles, M., Mercuri, A.M., Nomade, S., Nowaczyk, N., Panagiotopoulos, K., Peyron, O., Reed, J.M., Sagnotti, L., Sinopoli, G., Stelbrink, B., Sulpizio, R., Timmermann, A., Tofilovska, S., Torri, P., Wagner-Cremer, F., Wonik, T., Zhang, X., 2019. Mediterranean winter rainfall in phase with African monsoons during the past 1.36 million years. Nature 573, 256–260.

Wulf, S., Keller, J., Paterne, M., Mingram, J., Lauterbach, S., Opitz, S., Sottili, G., Giaccio, B., Albert, P.G., Satow, C., Tomlinson, E.L., Viccaro, M., Brauer, A., 2012. The 100–133 ka record of Italian explosive volcanism and revised tephrochronology of Lago Grande di Monticchio. Quat. Sci. Rev. 58, 104–123.

Wulf, S., Kraml, M., Brauer, A., Keller, J., Negendank, J.F., 2004. Tephrochronology of the 100 ka lacustrine sediment record of Lago Grande di Monticchio (southern Italy). Quat. Int. 122, 7–30.

Wulf, S., Kraml, M., Keller, J., 2008. Towards a detailed distal tephrostratigraphy in the Central Mediterranean: the last 20,000 yrs record of Lago Grande di Monticchio. J. Volcanol. Geoth. Res. 177, 118–132.

Zanchetta, G., Giaccio, B., Bini, M., Sarti, L., 2018. Tephrostratigraphy of Grotta del Cavallo, Southern Italy: insights on the chronology of Middle to Upper Palaeolithic transition in the Mediterranean. Quat. Sci. Rev. 182, 65–77.

Zhang, W., Hu, Z., 2020. Estimation of isotopic reference values for pure materials and geological reference materials. At. Spectrosc. 41, 93–102.